12-1-2013

Pennsylvanian to Cretaceous folds and thrusts in south-central Nevada: evidence from the Timpahute Range

Angela Giovanna Russo
University of Nevada, Las Vegas, russoa4@unlv.nevada.edu

PENNSYLVANIAN TO CRETACEOUS FOLDS AND THRUSTS

IN SOUTH-CENTRAL NEVADA:

EVIDENCE FROM THE TIMPAHUTE RANGE

by

Angela Giovanna Russo

Bachelor of Science
Northern Kentucky University
2007

A thesis submitted in partial fulfillment
of the requirements for the

Master of Science - Geoscience

Department of Geoscience
College of Sciences
The Graduate College

University of Nevada, Las Vegas
December 2013

THE GRADUATE COLLEGE

We recommend the thesis prepared under our supervision by

Angela Giovanna Russo

entitled

Pennsylvanian to Cretaceous Folds and Thrusts in South-Central Nevada: Evidence from the Timpahute Range

is approved in partial fulfillment of the requirements for the degree of

Master of Science - Geoscience

Department of Geoscience

Wanda J. Taylor, Ph.D., Committee Chair

Ganqing Jiang, Ph.D., Committee Member

Eugene Smith, Ph.D., Committee Member

Lon Spight, Ph.D., Graduate College Representative

Kathryn Hausbeck Korgan, Ph.D., Interim Dean of the Graduate College

December 2013

ABSTRACT

Pennsylvanian to Cretaceous folds and thrusts in south-central Nevada: evidence from the Timpahute Range

by

Angela Russo

Dr. Wanda J. Taylor, Examination Committee Chair
Professor of Geoscience
University of Nevada, Las Vegas

Understanding Permian and Mesozoic contractional structures from southern California to northern Nevada requires correlation through south-central Nevada. After the Devonian-Mississippian Antler orogeny through the Permian-Triassic Sonoma orogeny and then up to the Sevier orogeny, south-central Nevada was thought to have remained tectonically inactive. However, Pennsylvanian through Jurassic age deformation is documented to the south in Death Valley and to the north. Identifying geometries, spatial relationships, and relative timing of deformations in the Timpahute Range, south-central Nevada, is an essential piece to completing the overall understanding of Nevada geology. The purpose of this study is to identify and analyze deformational structures of the Timpahute Range and clarify their geometries, relative timing, regional correlation, and tectonic significance.

All contraction in the Timpahute Range is constrained by Antler foreland basin units and the intrusion of the 102.9 ± 3.2 Ma Lincoln stock. New mapping at a scale of 1:12,000 documents three contractional episodes in the Timpahute Range, and cross-cutting relations from this study determine at least a relative timeline. The Tempiute

Ridge Block contains a W-vergent fold that represents the earliest contractional event in the area. Next was the W-vergent Schofield Pass fault zone. The last contractional deformation formed E-vergent structures of the Central Nevada thrust belt which make up the Lincoln duplex.

In collisional orogens, closely related thrust faults may join together in a fault system that includes such structures such as imbricate fans and duplexes. The Lincoln duplex, part of the Central Nevada thrust belt exposed in the Timpahute Range and southern Worthington Mountains, consists of folds and a sequence of thrust faults. New data suggest the Lincoln duplex is a variation of the hinterland dipping duplex, with out-of-sequence thrusts.

Cenozoic extensional faults overprint the contractional structures. A series of NW-striking normal faults terminate at a major ENE-striking left-lateral strike-slip fault. This fault continues eastward through multiple ranges in south-central Nevada as part of the Timpahute lineament.

ACKNOWLEDGEMENTS

This research was partially supported by National Science Foundation Grant EAR-0150915 to Cashman, Trexler, Davydov, and Taylor; the UNLV Geoscience Bernada French Scholarship; and the UNLV Geoscience Nate Stout Memorial Scholarship. I owe many thanks to my committee chair and advisor Wanda Taylor, for everything she has taught me and giving me this amazing opportunity. To Wanda, you are a true mentor and friend. Thank you for your patience and never giving up on me. I appreciate the time and effort expended by my committee members, Ganqing Jiang, Gene Smith, and Lon Spight. Thank you to Rod Metcalf, Steve Rowland, and Janet Bertog for your guidance as well. Thank you to the University of Nevada Las Vegas Geoscience Department administrative assistants Maria Figueroa and Elizabeth Smith; I would have been lost without your help and support. Thanks to the community members of Rachel, Nevada for their hospitality. I benefited from discussions with many colleagues and friends, several of whom traveled to the Timpahute Range at some point: Pasquale Del Vecchio, Kevin Donahue, Jonathan Carter, James Thompson, Samuel Siebenaler, and Paul Kosmidis, miss you buddy. To Gavyn Salazar, for keeping me motivated; you will be a great geologist. Thank you CG for never letting me give up. I would like to thank my parents and supporters in Centerville, Cincinnati, Louisville, Las Vegas, and Winnemucca. Thank you to my brothers, Nick and Joe, who have always supported me. To Nicholas Russo, my field assistant, one of the greatest opportunities of this project was getting to map my field area with my brother. To my Grandma and Mike, thanks for believing in me, without you graduate school wouldn't have been possible.

TABLE OF CONTENTS

LIST OF FIGURES

CHAPTER 1

INTRODUCTION

Major deformations in south central Nevada from late Jurassic through early Cenozoic in age are attributed to the east-vergent Sevier orogenic belt and Central Nevada thrust belt (CNTB) (Fig. 1) (e.g., Armstrong, 1968; Taylor et al., 1993; DeCelles et al., 1995; Taylor et al., 2000; Long, 2012). Structures in the Timpahute Range, which are widely bracketed between Pennsylvanian and Cretaceous in age, were previously considered to be part of the CNTB and Sevier orogeny, because the region was thought to be tectonically inactive from Pennsylvanian through Jurassic time. However, some question remained about the timing of inconsistent and poorly documented structures in the western Timpahute Range (Cashman et al., 2008).

Pennsylvanian through Jurassic aged shortening is documented in Death Valley and southern Nevada, northern Nevada, and the Luning-Fencemaker belt of west-central Nevada (Figs. 1 and 2) (e.g., Oldow, 1983; Speed, 1983; Snow and Wernicke, 1989; Caskey and Schweickert, 1992; Cole and Cashman, 1999; Wyld, 2002; DeCelles, 2004; Trexler et al., 2004; Cashman et al., 2008; Cashman et al., 2011; Long, 2012). However studies of contractional structures through central Nevada are limited. With an increasing number of studies showing pre-Sevier aged deformation both north and south of the Timpahute Range (Fig. 1), it is plausible that some structures in the area may not be related to the CNTB but show whether this belt of deformation continues throughout the region.

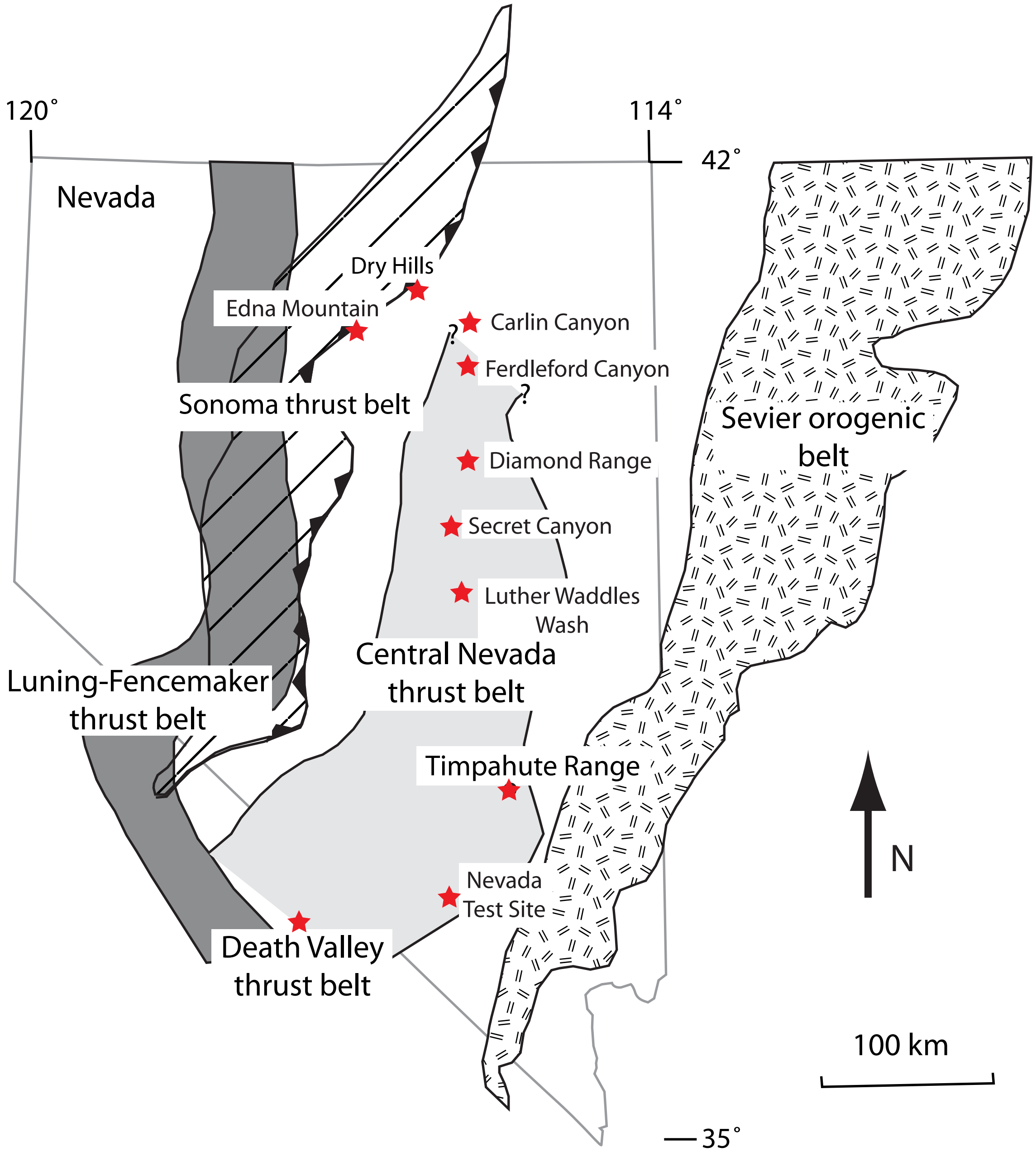

Figure 1. Mesozoic orogenic belts of Nevada and Pennsylvanian to Jurassic aged deformation. Modified from Snow and Wernicke (1989), Caskey and Schweickert (1992), Taylor et al. (1993), Dickinson (2006), Cashman et al. (2008), and Siebenaler (2010).

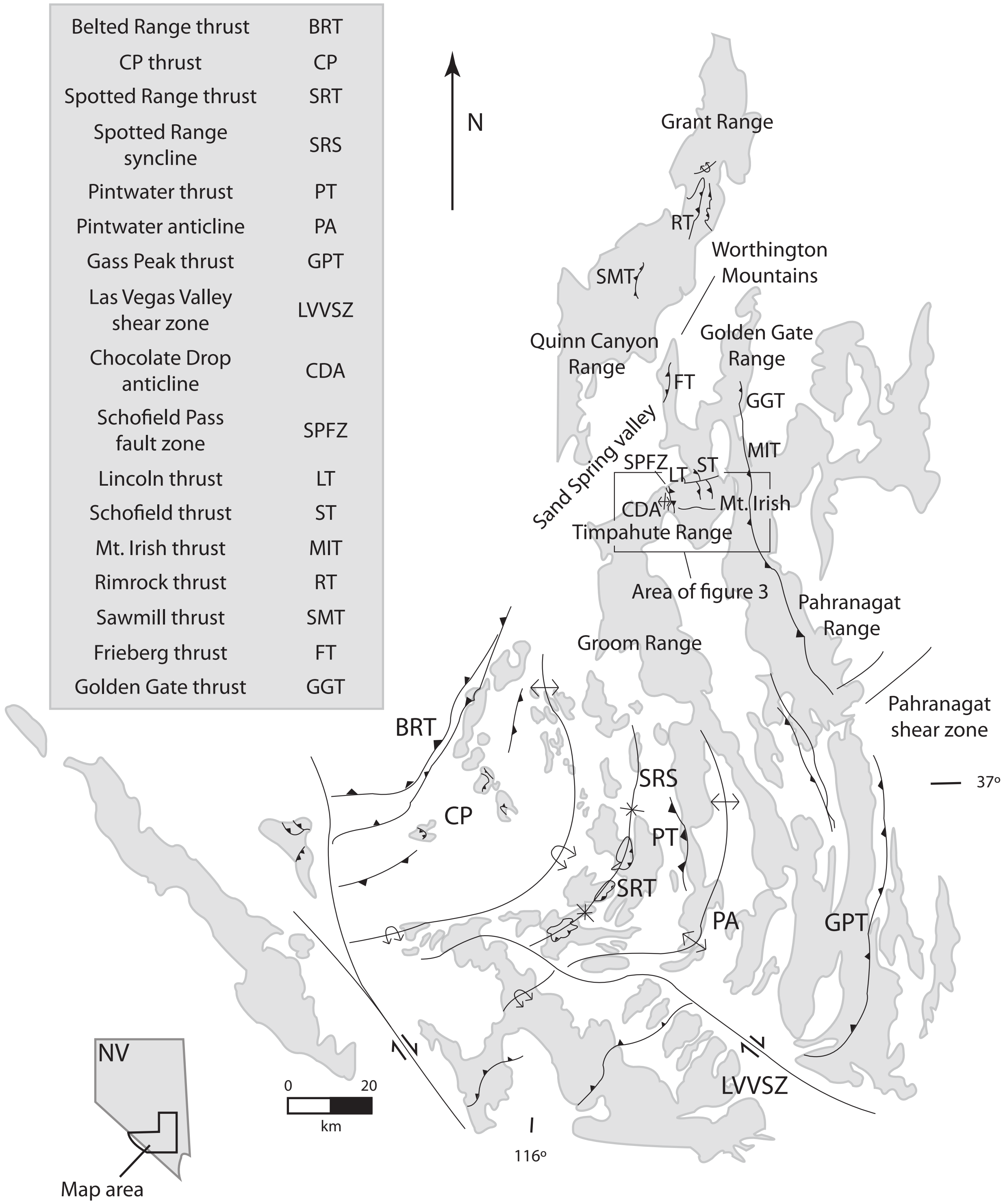

Figure 2. Regional structure map of south-central Nevada. Compiled from new mapping, Caskey and Schweickert (1992), and Taylor et al. (2000).

The purpose of this study is to evaluate the origin of structures that do not appear to fit with previously recognized deformation of the region; expand knowledge of thrust system structural development, specifically duplexes; and determine whether deformation occurred in the Timpahute Range prior to known CNTB deformation. To address these issues, I used new detailed geologic mapping (1:12,000 scale), structural analyses, and refined dates, from the western Timpahute Range, including the Tempiute Ridge block (TRB) and Lincoln duplex.

The folded TRB is intruded by the Cretaceous Lincoln stock (Fig. 3), which paleomagnetic data show is not tilted (Taylor et al., 2000), and is bound on the east by the Schofield Pass fault zone (SPFZ). Therefore, the folding of the TRB must have occurred prior to emplacement of the Lincoln stock suggesting deformation in the western Timpahute Range pre-dates the Sevier Orogeny and emplacement of the CNTB. Detailed field mapping and structural analysis revealed the SPFZ to have initially been a reverse fault active between the deposition of the Pennsylvanian Ely limestone and intrusion of the Lincoln stock (Fig. 3) and an earlier, separate structure from the CNTB.

Exposures of the Lincoln duplex, one of the CNTB structures exposed in the Timpahute Range, as well as the southern Worthington Mountains (Fig. 3) (Taylor et al., 1993; Taylor et al., 2000), suggest the structure is unlike the standard models of duplex development (Boyer and Elliot, 1982). Initial inspection of rock units, folds, and faults in the duplex suggests that the sequence of thrusting as well as the geometric configuration of individual horses is not consistent with classic end-member models of duplex

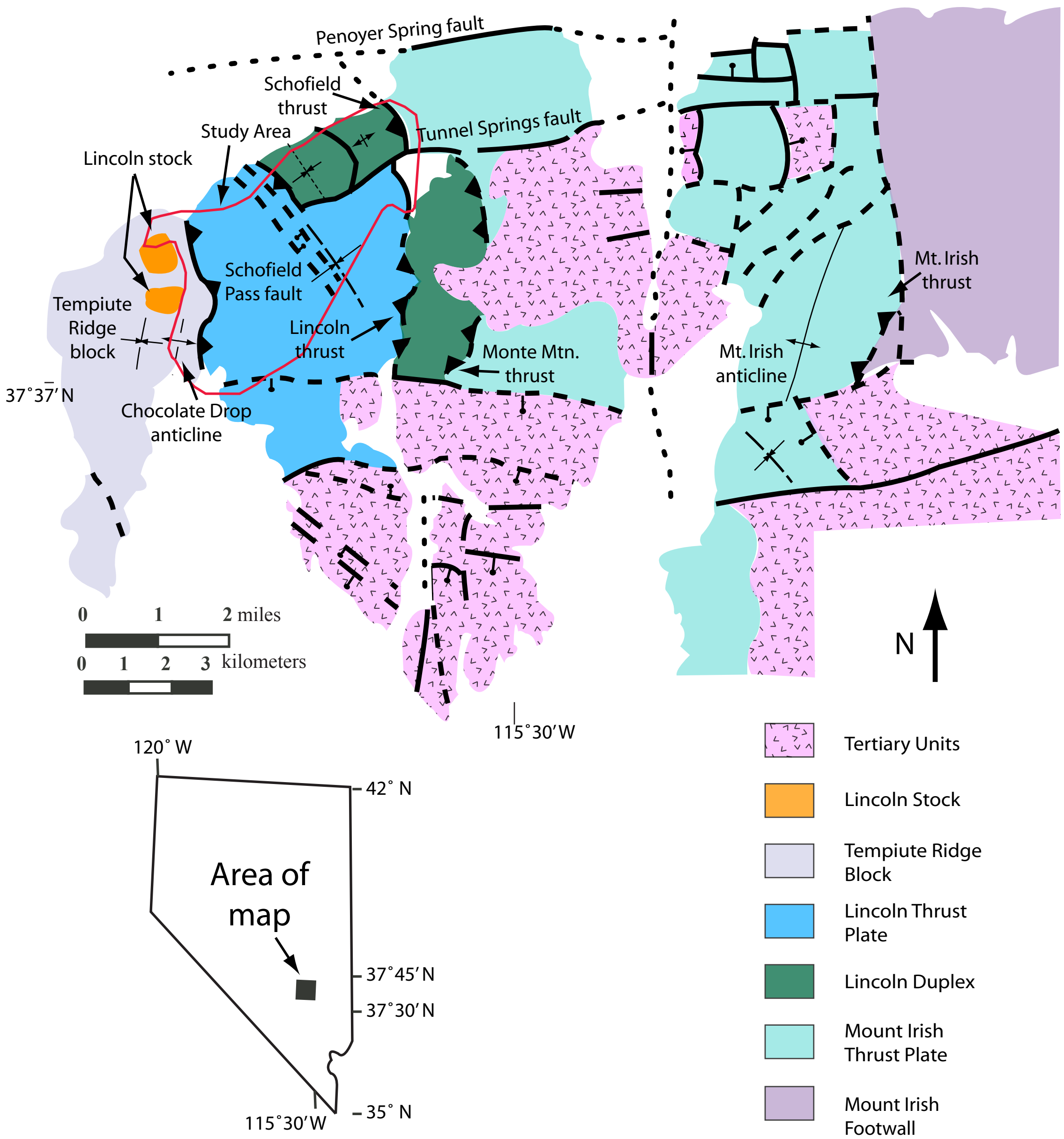

Figure 3. Tectonic map of the Timaphute Range and Mt. Irish showing major structures and the Lincoln stock. Compiled from new mapping, Taylor et al. (2000) and Bigdoli (2005).

formation but is more likely a variation, interpreted here as an out-of-sequence hinterland dipping duplex.

Contractional structures of the region have been overprinted (Fig. 3) and, in some cases reactivated, by Cenozoic extension (e.g., Wernicke, 1992). Detailed mapping and analysis of an ENE-striking fault and nearby high-angle normal faults show a transfer fault with a significant component of strike slip. This transfer fault can now be shown to offset some of the CNTB structures, and correlate regionally complicating structures of south-central Nevada.

CHAPTER 2

BACKGROUND

Plate interactions along the western edge of the North American plate led to an extensive tectonic history in Nevada (e.g., Burchfiel et al., 1992; Miller et al., 1992). This tectonic activity produced major contractional events, specifically the Antler, Sonoma, and Sevier orogenies and Cenozoic extension in the region (Fig. 1) (e.g., Armstrong, 1968; Speed and Sleep, 1982; Wernicke, 1992; Dickinson, 2006). In the Timpahute Range, the deformed strata include Paleozoic sedimentary rocks, ranging in age from Cambrian to Pennsylvanian, that are unconformably overlain by Cenozoic volcanic and sedimentary units.

In the early Paleozoic, the area that is now Nevada was part of a passive margin (miogeocline) influenced by sea level fluctuations (Armstrong, 1968; Speed and Sleep, 1982; Burchfiel et al., 1992). During this time, shallow water sediments, craton-derived and carbonate-bank, were deposited, thickening to the west (Burchfiel et al., 1992). Early Paleozoic units located in the study area include the Cambrian Bonanza King Formation or equivalent; the Ordovician Pogonip Group, Eureka Quartzite, and Fishhaven Dolomite; the Silurian Laketown Dolomite; and the Devonian Sevy Dolomite, Simonson Dolomite, and Guilmette Formation (Fig. 4) (Tschanz and Pampeyan, 1970; Miller et al., 1992; Taylor et al., 2000).

In the late Devonian to Mississippian, during the Antler orogeny, east-vergent thrusts formed the Roberts Mountain allochthon, which is exposed in modern day north-central Nevada (Speed and Sleep, 1982; Oldow, 1984; Miller et al., 1992). This deformation

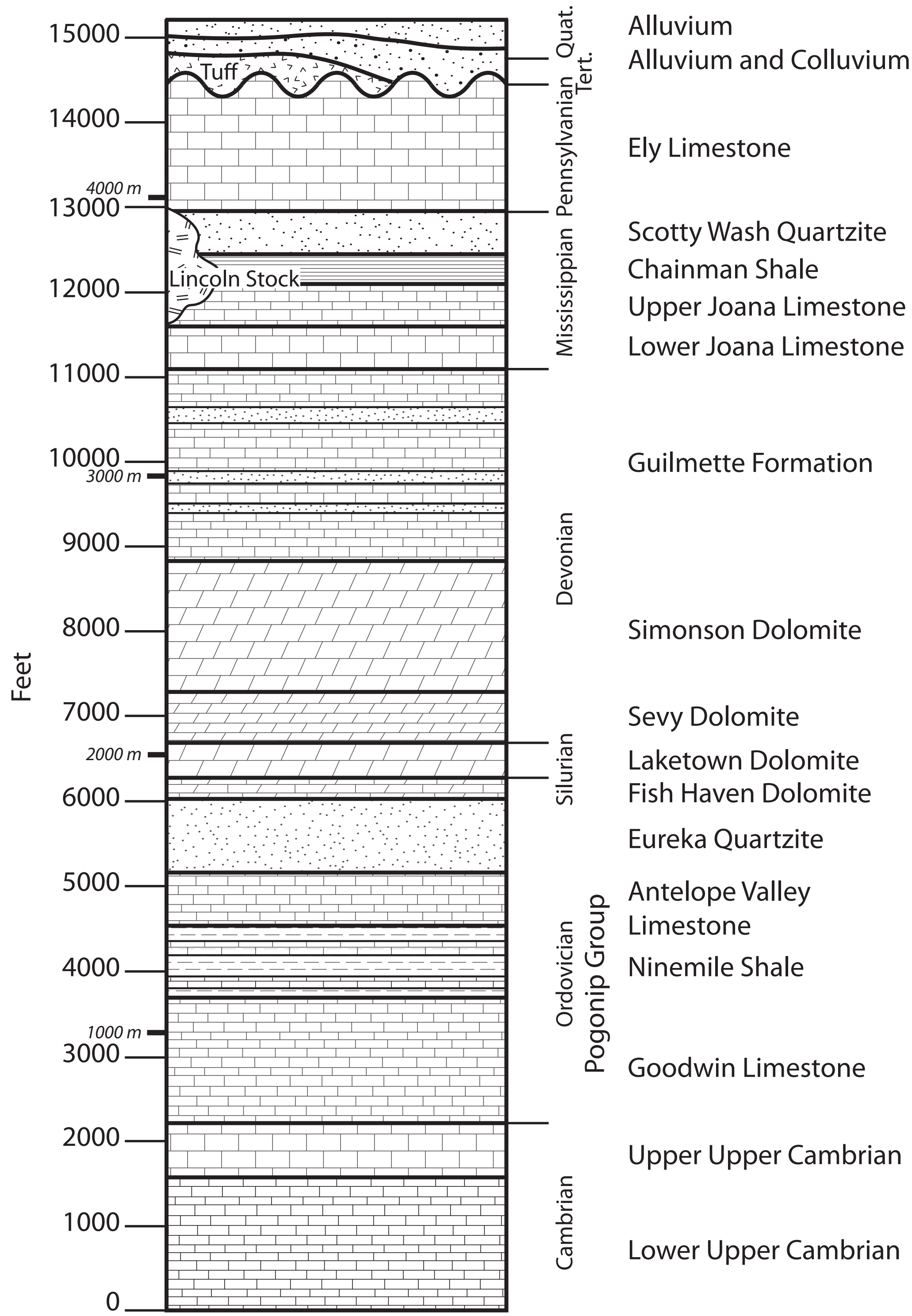

Figure 4. Stratigraphic section of the Timpahute Range. Standard lithologic patterns used. Lincoln Stock is Cretaceous in age. See Appendix A and Plate 1 for complete unit descriptions.

occurred throughout central Nevada causing modern day south-central Nevada to subside as part of the Antler foreland basin. The foreland-basin units exposed in the Timpahute Range include the Mississippian Pilot Shale (upper part), West Range Limestone, Joana Limestone, Chainman Shale, and Scotty Wash Quartzite (Fig. 4) (Tschanz and Pampeyan, 1970; Miller et al., 1992; Taylor et al., 2000).

In the Pennsylvanian, the Ely Limestone (Fig. 4) was deposited in a shallow marine basin; this basin succeeded the Antler foreland basin (Saller and Dickinson, 1982). This unit is interpreted as a part of the Antler Overlap Sequence (Roberts et al., 1958; Poole, 1974; Dickinson, 2006).

From the end of the Pennsylvanian through the end of the Triassic, the region around the Timpahute Range is typically considered to have remained tectonically inactive, with limited influence by the Sonoma orogeny (Fig. 1). The Permo-Triassic Sonoma orogeny emplaced the Golconda allochthon (Fig. 1), which contains sedimentary units of the Havallah basin, atop the continental shelf, in western Nevada (Miller et al., 1992; Dickinson; 2006). Speed (1983) noted that little deformation and thermal effects were imposed on rocks below the Golconda allochthon. Shallow marine carbonates are dominant east of the Sonoma orogenic belt (Burchfiel et al., 1992); however none are preserved in the field area.

More recently, studies have shown contractional structures between Pennsylvanian and Cretaceous in age south of the Timpahute Range in the Nevada Test Site (now called Nevada National Security Site) (Guth, 1981; Guth, 1990; Caskey and Schweickert, 1992; Cole and Cashman, 1999; Long, 2012) and into Death Valley (Snow, 1992; Snow and

Wernicke, 1989). These include the west-vergent CP thrust, and the east-vergent Spotted Range thrust and Belted Range thrust (see table 1). The Belted Range thrust is interpreted as late Permian to pre-middle Triassic; Snow (1992) mapped the thrust cross cutting intrusive rocks in the Cottonwood Mountains and intruded by rocks as young as 102 Ma (Cole et al., 1993). The Belted Range thrust is correlated to the Last Chance thrust system in Death Valley (Snow and Wernicke, 1989; Caskey and Schweickert, 1992; Cole and Cashman, 1999; Long, 2012) which is late Triassic to early Jurassic in age (Figs. 1 and 2).

From the Jurassic to the Cenozoic, western North America experienced multiple deformational events (Fig. 1). The first of these contractions formed the Luning-Fencemaker thrust belt which displays hundreds of kilometers of major, generally Jurassic, shortening between a volcanic arc, to the west, and the continental shelf, to the east (Oldow, 1983; Wyld et al., 2001; Wyld, 2002; Wyld et al., 2003). The Luning-Fencemaker thrust belt is exposed in western Nevada and consists of east-vergent thrusts and intensely deformed Triassic and Jurassic marine sediments (e.g., DeCelles, 2004). Speed (1983) and Oldow (1983) suggested a common decollement linking the Luning-Fencemaker thrust belt and Sevier belt, between which lay an area of minimal shortening. However, recent research suggests this deformation is independent from the slightly younger CNTB, Eureka thrust belt, and Sevier belt (Wyld et al., 2001; Wyld, 2002; DeCelles, 2004).

Late Jurassic to middle Paleogene deformation in the western United States is marked by the Sevier orogeny. This contractional event formed dominantly east-vergent folds and thrusts from southern California and Nevada, through central Utah, northward into southern Canada (Fig. 1) (e.g., Armstrong, 1968; DeCelles, 2004). Major thrusts of the Sevier orogeny typically have a ramp-flat geometry (Wernicke et al., 1988) and generally young eastward, placing older thrusts structurally higher than younger thrusts (Armstrong, 1968; Axen et al., 1990; Cowan and Bruhn, 1992). Armstrong (1968) described the frontal thrust of the Sevier belt as thin-skinned contraction; however some studies have shown the local inclusion of basement rocks (Burchfiel and Davis, 1972; Yonkee, 1992; DeCelles et al., 1995; DeCelles, 2004). Timing of the Sevier orogeny remains a subject of research, however the event is normally constrained between late Jurassic to Eocene (e.g., DeCelles et al., 1995; Taylor et al., 2000) based on structural and sedimentological evidence. Thus, this belt possesses at least minimal timing overlap with the aforementioned Luning-Fencemaker thrust belt (Oldow, 1983; Speed et al., 1988; Wyld et al., 2003).

Modern day south-central Nevada is located in the hinterland of the Sevier orogenic belt (Fig. 1) (e.g., Armstrong, 1968; Allmendinger and Jordan, 1984; Taylor et al., 2000). Early interpretations of hinterland deformation suggest broad gentle folds, extensive ductile deformation (e.g., Armstrong, 1968, 1972), low-angle faults, and only minor offset (e.g., Armstrong, 1968; Oldow, 1983; Allmendinger and Jordan, 1984) at deeper structural levels or during subsequent deformations (Armstrong, 1972). However, subsequent studies (e.g., Taylor et al., 2000; Long, 2012) show that significant deformation occurred west of the frontal Sevier belt. In this area, the CNTB / Eureka belt have been linked to the Sevier orogeny and partly incorporate the same structures (Fig. 1)

(Speed, 1983; Speed et al., 1988; Taylor et al., 2000). However, the location, age, and relationships among the CNTB, Eureka belt, and Sevier belt remain controversial.

The CNTB is a ~north-south striking system of contractional folds and faults in south-central Nevada, exposed in at least nine ranges from Alamo to Eureka, including the Timpahute Range (Fig. 1) (Taylor et al., 1993; Taylor et al., 2000; DeCelles, 2004). The timing of the CNTB is widely bracketed from Permian to mid-Cretaceous (Taylor et al., 1993; Taylor et al., 2000) based on the youngest units found in fault blocks, cross-cutting relations, and mid-Cretaceous intrusions which post-date contraction. The CNTB was interpreted by Taylor et al. (1993) to include pre-Cenozoic contractional structures, east of the Fencemaker allochthon, exposed in strata as young as Permian (Fig. 1). Structures of the CNTB exposed in the Timpahute Range are typical of a thrust belt and include thrust faults, backthrusts, large upright and overturned folds, and a duplex (Taylor et al., 1993).

Mapping of the Garden Valley thrust system (Figs. 2 and 3), including structures exposed in the Timpahute Range, places it within the CNTB (Taylor et al., 2000). Taylor et al. (2000) state that part of the Garden Valley thrust system, the Mt. Irish-Golden Gate thrust, correlates to the Gass Peak thrust of southern Nevada, previously attributed to and widely accepted as part of the Sevier belt (e.g., Armstrong, 1968; Guth, 1981; Burchfiel et al., 1992; DeCelles and Coogan, 2006). Furthermore, documented timing of deformation within the CNTB overlaps the age brackets of the Sevier thrust belt. Therefore, Taylor et al. (2000) interpret the CNTB as a structurally-linked, internal branch of the Sevier thrust belt.

The TRB lies in the western part of the Timpahute Range, contains folded strata and is bound on the east by the SPFZ, previously called the Schofield Pass fault (Fig. 3) (c.f., Tschanz and Pampeyan, 1970). The SPFZ juxtaposes Pennsylvanian and Mississippian rocks of the TRB against Ordovician and Cambrian units. The TRB is intruded by the Cretaceous Lincoln stock (Fig. 3), which paleomagnetic data show is not tilted (Taylor et al., 2000). Therefore, the folding of the TRB must have occurred prior to emplacement of the Lincoln stock. This relation may suggest deformation in the western Timpahute Range pre-dates the Sevier Orogeny and emplacement of the CNTB. A geometric link of these structures to the CNTB is questionable.

Igneous intrusions, such as the Lincoln stock, are documented within south-central Nevada (Fig. 3) (e.g., Bartley and Gleason, 1990; Barton, 1990; Taylor et al., 2000). The Lincoln stock is a quartz monzonite (Ekren et al., 1977) that paleomagnetic data indicate is untilted (Taylor et al., 2000). To provide an upper timing bracket for thrusts within the CNTB, Taylor et al. (2000) dated the Lincoln stock, using U/Pb TIMS, as mid-Cretaceous, at 98 ± 81 Ma. This work improves upon that date using U/Pb ion microprobe techniques (see below).

During the Cenozoic, widespread extension occurred and a series of rhyolitic to dacitic calderas formed (e.g., Stewart, 1980a; Best et al., 1989; Best et al., 1993). During this time, several thousand cubic kilometers of ash-flow deposits (tuffs) were unconformably emplaced atop exposed rocks, typically Paleozoic in age. Ash-flow tuffs exposed near the Timpahute Range were erupted from the Caliente and Central Nevada caldera complexes and are Oligocene to Miocene in age (e.g., Best et al., 1989; Taylor et al., 1989; Best et al., 1993; Bidgoli, 2005; Long, 2012). Cenozoic normal faults in Nevada are both low angle and high angle, generally striking north-south (e.g., Stewart, 1971; Wernicke, 1992). Pre-, syn, and post-volcanic normal faults are known (Stewart, 1971; Eaton, 1982; Wallace, 1984; Gans et al., 1989; Wernicke, 1992; Gans and Bohrson, 1998). However, synvolcanic and postvolcanic east-west striking faults with steep dips occur in discrete zones as well (e.g., Rowley, 1998; Taylor and Switzer, 2001; Bidgoli, 2005).

Prevolcanic extension occurred during two intervals: late Mesozoic to middle Eocene (e.g., Vandervoort and Schmitt, 1990; Wells et al., 1990; Hodges and Walker, 1992; Wells et al., 1998) and late Eocene to Oligocene (e.g., Jayko, 1990; Taylor and Bartley, 1992; Axen et al., 1993; Taylor and Switzer, 2001). Initial extension occurred in the Sevier hinterland alongside shortening, and is well-documented specifically in north-central Nevada, northwestern Utah, and southwestern Idaho (e.g., Wells et al., 1990, 1998; Hodges and Walker, 1992). Widespread Eocene to Oligocene extension occurred in two north trending belts (Wernicke,1992; Axen et al., 1993; Taylor and Switzer, 2001).

Initial postvolcanic faulting occurred during the late Miocene and Pliocene and accommodated both east-west extension and north-south extension (e.g., Taylor et al., 1989; Taylor, 1990; Best and Christiansen, 1991; Taylor and Switzer, 2001). North-south-striking faults developed in response to plate interactions (e.g., Severinghaus and Atwater, 1990; Bohannon and Parsons, 1995).

Transverse faults (e.g., Ekren et al., 1976; Rowley, 1998; Taylor and Switzer, 2001) formed in two different ways. (1) They resulted from a southward movement of crustal material which accompanied a large gravitational potential energy gradient associated with a migrating volcanic belt (Wernicke et al., 1988; Wernicke, 1992; Bidgoli, 2005). This gradient developed due to a contrast thermally elevated and magmatically thickened crust in the northern Great Basin, in addition to temporal and spatial differences in extension (Bidgoli, 2005). (2) They allowed differences in amount, style or magnitude of strain on opposite sides, in other words, they are accommodation zones and / or transfer faults (e.g., Faulds and Varga, 1998).

Transverse faults form east-west trending features known as lineaments (e.g., Timpahute lineament, etc.) (Fig. 5) (e.g., Ekren et al., 1976; Rowley, 1998). Faults of the Timpahute lineament are high angle, east-west-striking normal and northeast-striking oblique-slip faults, which are documented in the Hiko Range, Timpahute Range, and Mount Irish Range (Fig. 2) (Rowley, 1998; Taylor et al., 2000; Taylor and Switzer, 2001; Bidgoli, 2005).

Active faults that cut Quaternary deposits denote the most recent Basin and Range extension which began in the Pliocene and continues today. However, no Quaternary faults are exposed in the study area.

Background on Duplex Models

Boyer and Elliot (1982) described three styles of duplexes. These styles are the hinterland dipping duplex, the foreland dipping duplex, and the antiformal stack (Fig. 6). The hinterland dipping duplex contains horses which young in the direction of the frontal ramp. These horses dip toward the hinterland, and displacement along subsidiary faults is less than the length of the horse (Boyer and Elliot, 1982). In the foreland dipping

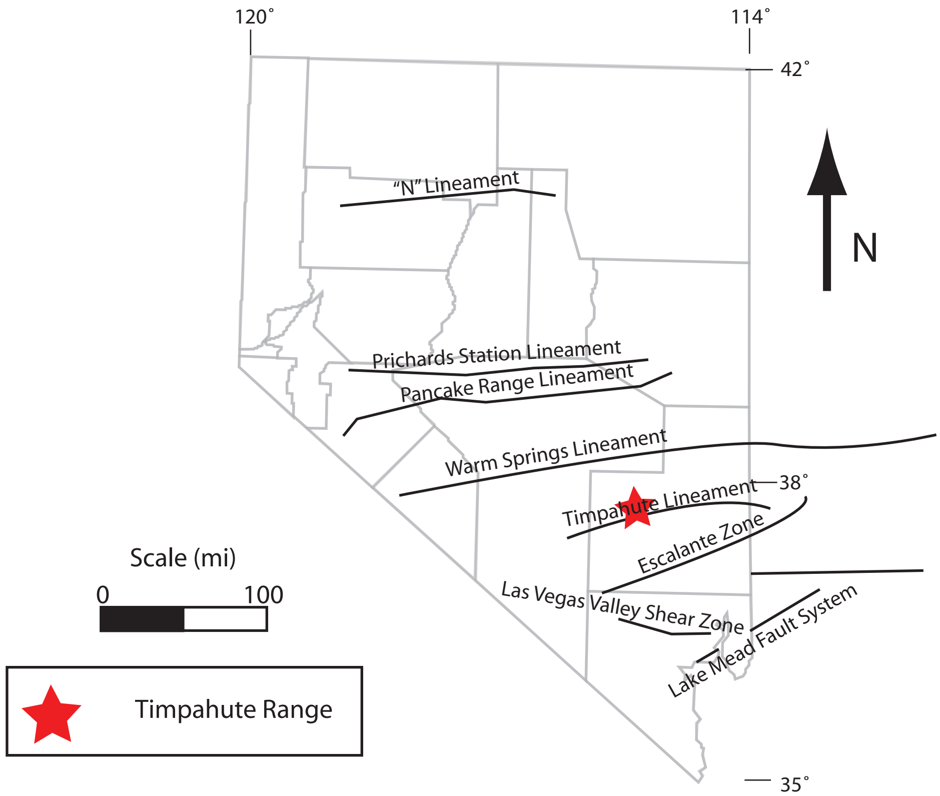

Figure 5. Post-volcanic (Oligocene - Miocene) lineaments in Nevada. Modified from Taylor and Switzer (2001).

duplex, the distance of transport of the horses is greater than the length of the horse. These horses dip in the direction of movement (toward the foreland) and young toward the hinterland (Boyer and Elliot, 1982). The antiformal stack is where the length of internal horses/slices is approximately equal to the amount of thrust slip which forms a bunching of branch lines and causes the older horses (upper) to fold about the younger horses (lower) (Boyer and Elliot, 1982). The Lincoln Duplex, of the Timpahute Range, does not appear to precisely match these models of duplex development. These models provide a context in which to consider the complexities observed in the lincoln duplex. The difference between the Lincoln duplex and the models could be due to either older structures being cut, offset and / or folded in the duplex or that the duplex formed in a manner somewhat unlike the classic models. Data and analysis suggest that the latter is the correct option.

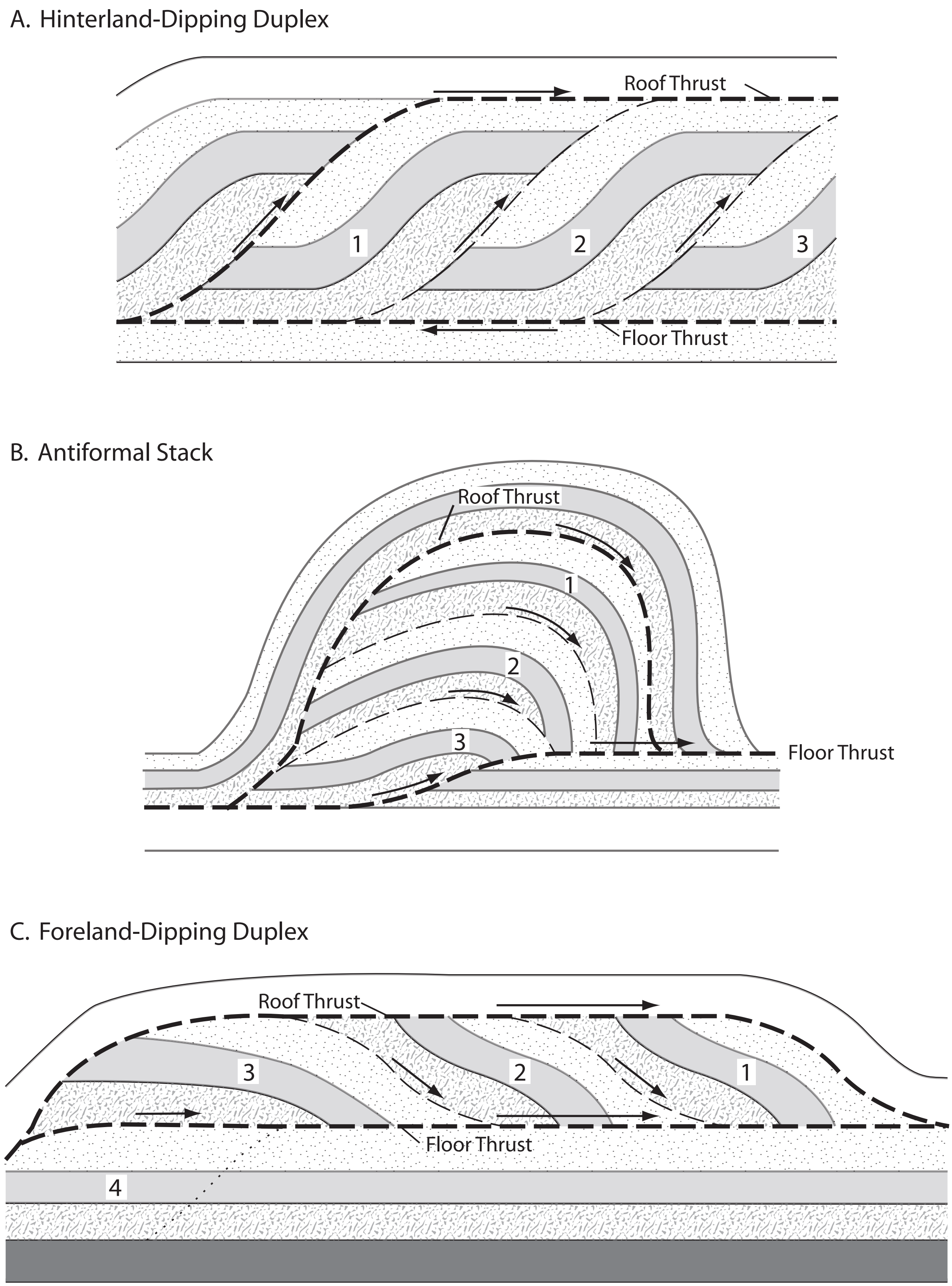

Figure 6. Models of duplex development. A, B, and C show different styles of duplex development. Modified from Boyer and Elliot (1982).

CHAPTER 3

METHODS

A geologic map of the field area was necessary for identifying structural geometries, cross-cutting relations, regional deformational events, and associated structures (Fig. 7, Plates 1 and 2). A field area of approximately 30 square kilometers was mapped at a scale of 1:12,000 using the 7.5 minute USGS topographic quadrangles of Monte Mountain, Tempiute Mountain North, Tempiute Mountain South, and Tempiute Mountain SE as a base (Fig. 3). Standard geologic mapping techniques (Compton, 1985) were used in identifying and recording rock units and contacts, unconformities, faults, folds, and intrusions. A Brunton® compass was used to measure the orientations of folds, faults, and beds in the units.

Stereographic projection was used to analyze the number and orientations of deformations. Stereograms were used to classify similar structures into kinematically compatible sets.

Retrodeformable cross sections were constructed (e.g., Dahlstrom, 1969; Groshong, 1989) to depict and analyze the structural history of the western Timpahute Range. These cross sections are an integral tool in comparing deformation of the Timpahute Range to regional deformation.

U/Pb SIMS geochronology was used to determine the age of the Lincoln Stock. Samples consisted of approximately 15 kg of rock and locations are shown on Plate 1. Zircons were extracted from this quartz monzonite using standard mineral separation techniques. Stock material was crushed and sieved then underwent magnetic separation

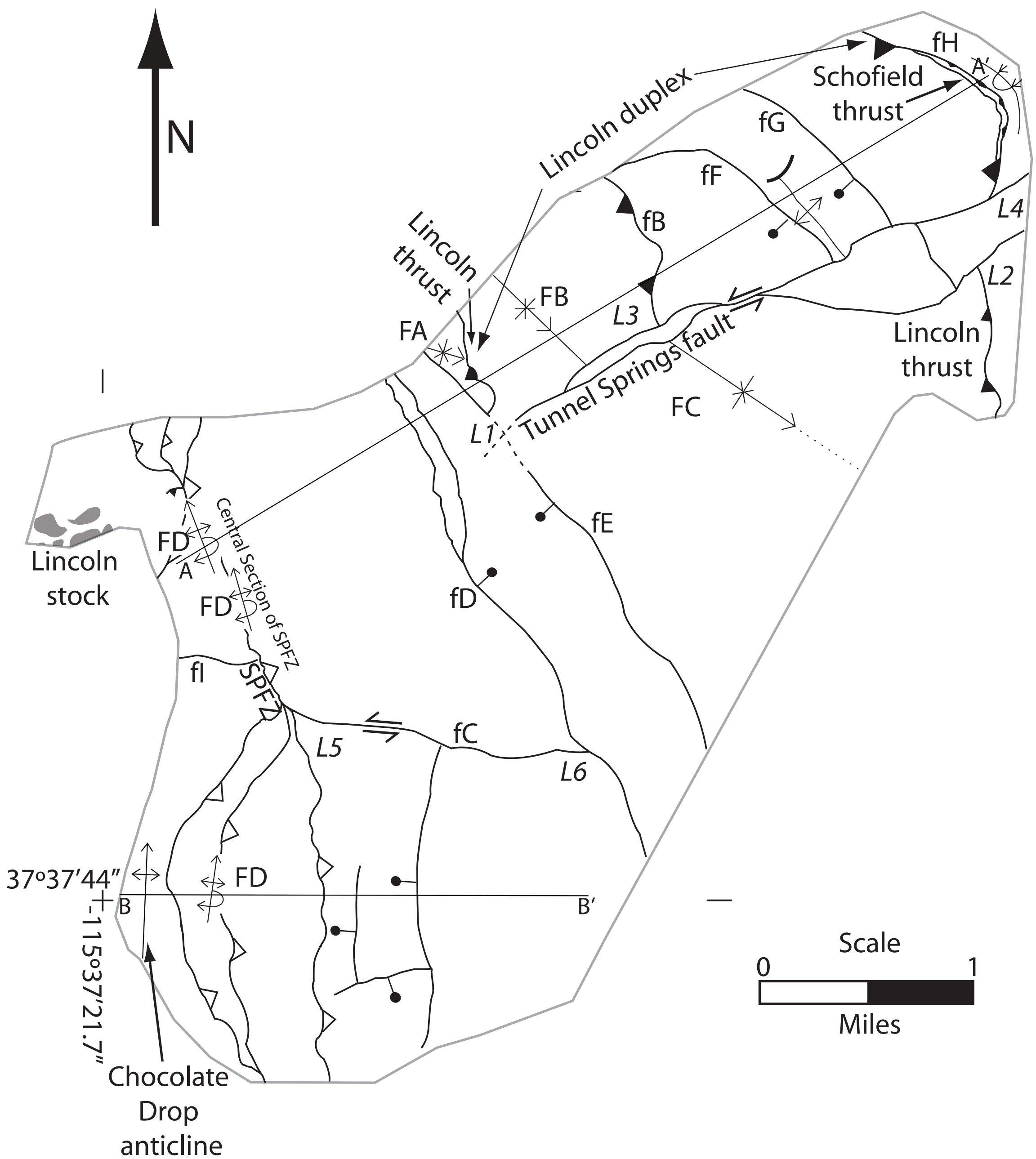

Figure 7. Simplified map showing structures identified in the study area, their names, and the geometric relations. f = Fault, F = Fold, and L = Location. Open teeth on thrust faults indicate W-vergent structures and solid teeth indicate E-vergent structures. The GPS coordinates shown are for Chocolate Drop, a landmark in Lincoln County.

followed by heavy liquid separation. Zircon grains were then hand selected under a microscope. U/Pb dates were obtained using the UCLA Cameca ims 1270 ion probe. Grains were mounted and analyzed following techniques as described in Schmitt et al. (2003).

CHAPTER 4

DATA

Stratigraphy

The stratigraphy of the Timpahute Range includes Upper Cambrian through Pennsylvanian marine carbonate, quartzite, and shale; a Tertiary tuff and Quaternary alluvial units (Fig. 4). Unlike the well-exposed Ordovician through Mississippian stratigraphy of the nearby Mt. Irish Range (Tschanz and Pampeyan, 1970), a complete section is not exposed in the area due to faulting and erosion. The lithologies and mapped formation contacts of the Upper Cambrian units, Ordovician Pogonip Group, and unnamed Mississippian Limestone of the study area have been modified from the Paleozoic stratigraphy of Nolan et al. (1956), Reso (1963), and Tschanz and Pampeyan (1970).

The uppermost Cambrian was divided into two subunits based on lithology (Fig. 4). The lower subunit, Lower Upper Cambrian, is at least 1600 ft (488 m) and characterized by dark and light striped moderately thick bedded limestone (See Plate 1, Appendix A for a more detailed description). The upper subunit, Upper Upper Cambrian, is a massive grey limestone with chert layers that is approximately 600 ft (183 m) thick (Plate 1, Appendix A). These subdivisions allow for better identification of faults because the relatively thin units allow smaller offset faults to be recognized.

The Ordovician Pogonip Group was divided into three formations that resemble those in the Eureka area: the Goodwin Limestone, Ninemile Formation, and Antelope Valley Limestone (Fig. 4) (Nolan et. al., 1956; Ross, 1964). This stratigraphy differs from the five subdivisions of the nearby Egan Range (Kellog, 1964) but better matches the exposures and rock types of the study area.

The unnamed Mississippian limestone of Tschanz and Pampeyan (1970) has been divided into two subunits here called Upper and Lower Joana Limestone (Fig. 4, Plate 1, Appendix A). However, in this case, the name is not as important as the division of the two units, again, because thin units aid in the definition of smaller offset faults. The Lower Joana Limestone consists of a massive cliff-forming limestone, which is abundant in large (1-2 cm) crinoid stems in eastern exposures while the exposures of the TRB contain mollusks, bryozoans, and fewer, small crinoids. The Upper Joana Limestone is a thin-bedded slope former. Regional thickness of the unnamed Mississippian limestone is 1000 ft (305 m) (Tschanz and Pampeyan, 1970); given exposures in the area, the upper and lower units have been estimated at 500 ft (152 m) each.

An red-purple, welded ash-flow tuff with feldspar and quartz phenocrysts is exposed in the northern field area. However, it is too altered to identify the unit.

Dates of Lincoln Stock

A small equigranular quartz monzonite intrusion associated with tungsten skarn deposits is exposed in the northwestern part of the map area. This intrusion, the Lincoln stock, has been suggested to be a variety of ages from Cretaceous to Tertiary (Tschanz and Pampeyan, 1970; Krueger and Schilling, 1971; Ekren et al., 1977; Tingley, 1991; Taylor et al., 2000). Previous U/Pb TIMS dating showed marked variability in the zircons (Taylor et al., 2000). Mineral separations indicated the percentage of zircons in the stock is low, <<1%. U/Pb analyses performed at UCLA's ion microprobe lab yielded weighted mean dates of 109 ± 12 Ma and 102.9 ± 3.2 Ma (Fig. 8, Appendix B). Due to the limited amount of zircons, multiple analyses were carried out on each grain to yield a smaller uncertainty. Standard errors are small and age distributions overlap significantly for five of the analyses (Figs. 8a and 8c). The weighed mean date of 102.9 ± 3.2 Ma has the smallest uncertainty and the best mean square weighted deviation (MSWD), so that value is preferred here (Figs. 8a and 8c).

Metamorphism

A zone of metamorphism was mapped around the Lincoln stock. The zone continues for about 1.06 km to the east and at least 0.61 km to the north of exposed stock, which lies in the northwestern edge of the map area. The western edge of the metamorphism is outside of the map area. The exposed units that are metamorphosed are Lower Upper Cambrian, Devonian Guilmette Formation, Mississippian Lower and Upper Joana limestones, and Mississippian Chainman Shale. The metamorphism varies from slate in the Chainman Shale to moderately-highly crystalline marbles in the carbonate units.

Faults

The rocks of the Timpahute Range underwent multiple periods of deformation, both contractional and extensional. The new mapping shows four fault sets: east-west striking faults, northwest-striking normal faults, northwest-striking thrust faults, and the north-striking SPFZ.

Four northwest-striking, northeast-directed thrust faults are located in the eastern portion of the map area. These faults include the Lincoln thrust, fault B, the Schofield thrust, and fault H (Figs. 7 and 9, Plates 1 and 2).

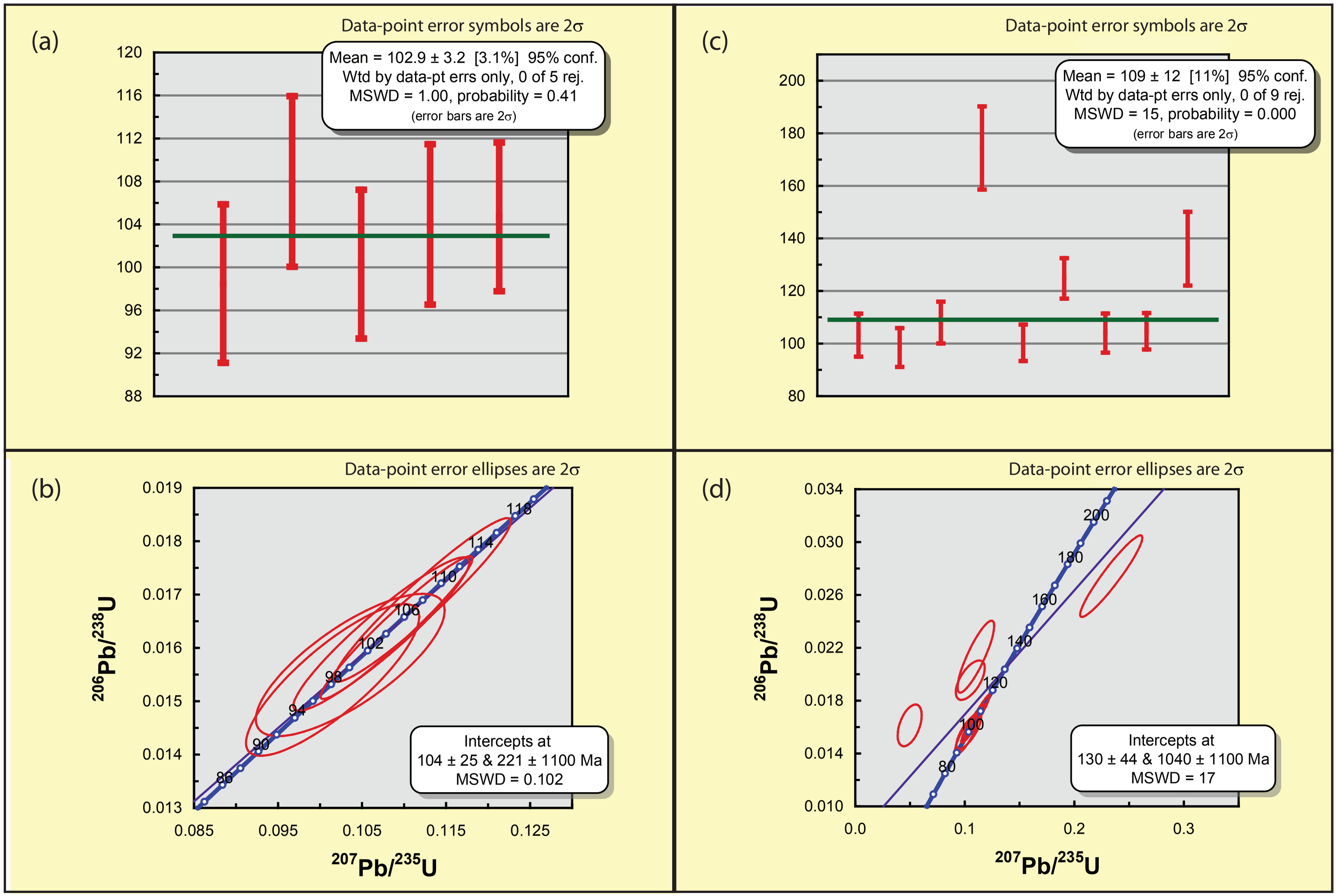

Figure 8. U/Pb weighted mean dates and concordia diagrams plotted from samples of the Lincoln stock. Graphs a and b show the same data points. Graphs c and d show the same data points and include the data in a and b. The date of 102.9 ± 3.22 Ma from graph a is preferred because of the smaller uncertainty and reasonable MSWD (mean square weighted deviation).

The Lincoln thrust strikes 133° and dips 60° SW at one measured location, which is consistent with calculated values. This fault juxtaposes the Ordovician Pogonip units and Eureka Quartzite with the Devonian Guilmette and Simonson formations, and the Mississippian Lower Joana Limestone (Fig. 9, Plate 2). The angle between the fault surface and footwall beds is 75° making this section a footwall ramp. Due to the presence of additional faults, the angular relationship between the thrust and beds of the hanging wall is uncertain. The Lincoln thrust terminates at the Tunnel Springs fault, at locations 1 and 2 (Fig. 7, Plate 1).

Fault B is a thrust fault which strikes northwest and dips to the southwest, but is largely concealed by alluvium. This fault places Devonian Simonson Dolomite and Guilmette Formation over Mississippian Upper Joana Limestone (Fig. 9, Plate 2). Fault B terminates against the Tunnel Springs fault, at location 3 (Fig. 7, Plate 1).

The Schofield thrust is a northwest-striking, southwest-dipping fault that places Devonian Guilmette Formation atop the Mississippian Lower Joana Limestone. It has a measured orientation of 148°, 11°SW. The Schofield thrust terminates against the Tunnel Springs fault, at location 4 (Figs. 7 and 9, Plates 1 and 2).

Fault H is a low-angle, northwest-striking reverse fault that places Mississippian Lower Joana Limestone atop the Chainman Shale. This fault has a calculated attitude of 157°, 7°SW (Figs. 7 and 9, Plates 1 and 2).

Two northwest-striking normal faults are exposed, fault D and fault E (Fig. 7, Plate 1). Fault D splays to the north and breccia zones along the fault show a northeast dip. This fault juxtaposes Devonian Simonson Dolomite, Guilmette Formation and

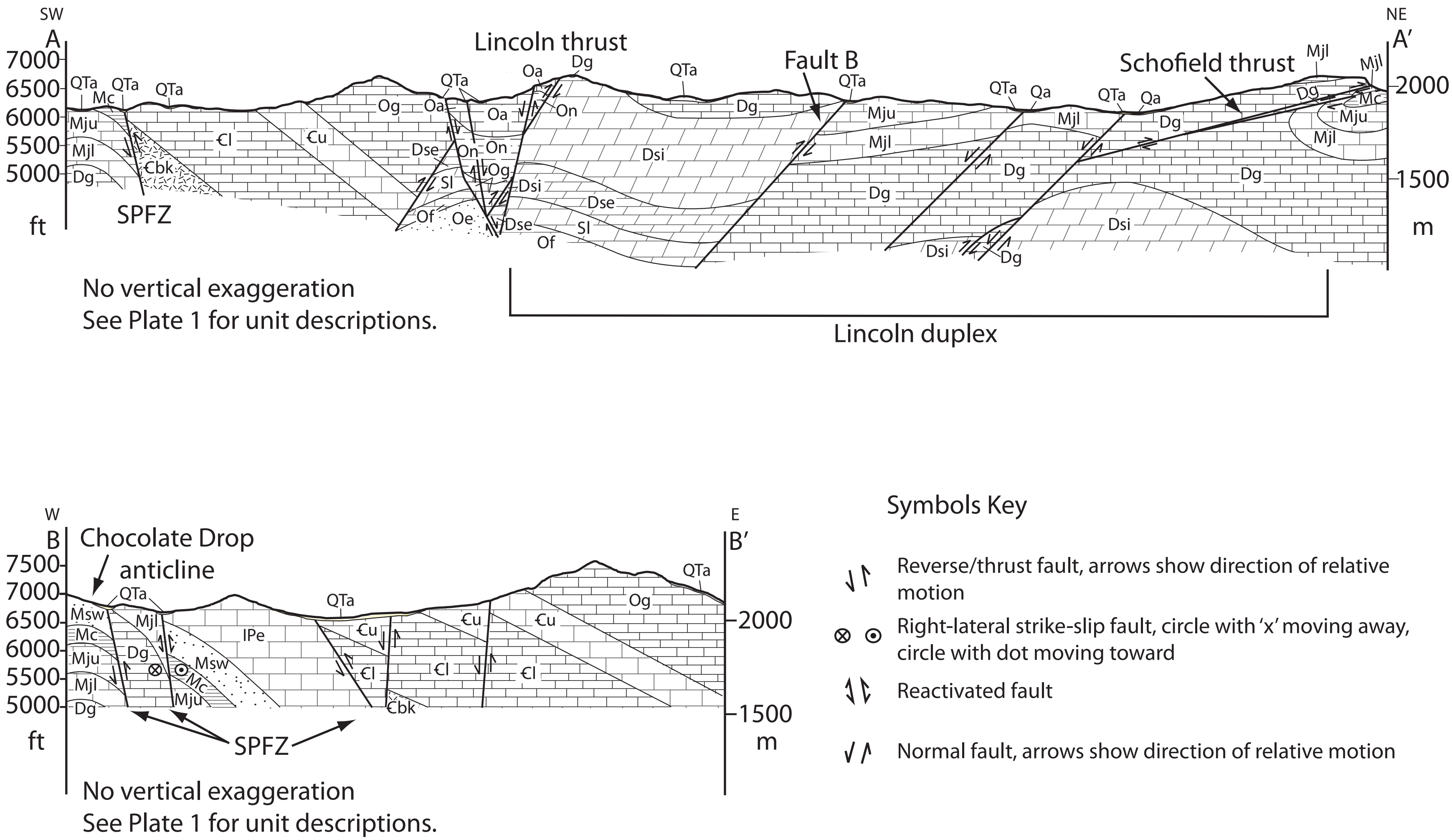

Figure 9. Geologic cross sections of the western Timpahute Range. Cross section A-A’ in the northern Timaphute Range, crosses SPFZ and Lincoln duplex. Cross section B-B’ in the southern Timpahute Range, crosses splays of the SPFZ.

Mississippian Joana Limestone against Ordovician Pogonip Group and Eureka Quartzite (Fig. 9, Plate 2). Fault E dips to the southwest and is poorly exposed but is identifiable due to offset between units when projected across the concealed zone and traced along the hillside. The geometry and amount of extension appear to differ north and south of the intersection (Location 1) with the Tunnel Springs fault (Fig. 7).

Normal faults F and G are located in the northeast section of the map and terminate at the Tunnel Springs fault (Fig. 7, Plate 1). Both are buried by Quaternary alluvium, but cut across strikes of beds and fold hinges and are noted by excessive stratigraphic separation in units exposed on opposite sides of the alluvium. Fault F juxtaposes Mississippian Lower Joana Limestone next to even lower Lower Joana Limestone while fault G places Lower Joana Limestone next to Devonian Guilmette Formation. Both faults cut pre-existing folds (Fig. 9, Plate 2).

A single northeast-striking fault is exposed in the map area, here called the Tunnel Springs fault. The Tunnel Springs fault is a steeply dipping fault which splays to the east and ends on the west near fault E at location 1 (Fig. 7). This fault is an apparent left-lateral fault and offsets the Lincoln and Schofield thrusts, as well as units of their respective hanging walls and footwalls by 12,400 ft, or 2.3 miles (3.8 km) (Fig. 7, Plate 1). Folds in the area are not continuous across the Tunnel Springs fault.

Fault C is a steeply dipping fault which strikes east-west to WNW from location 5 to location 6 (Fig. 7, Plate 1) and is buried by alluvium. This fault is identifiable by offset of the Cambrian and Ordovician outcrops to the north and south of the alluvium when projected along strike. Fault C has apparent left-lateral slip indicated by the offset of Cambrian and Ordovician units to the north and south.

Fault I is a steeply dipping EW-striking fault which cuts across the TRB and terminates at the SPFZ (Fig. 7, Plate 1). This fault is buried by alluvium and mainly identifiable by structural differences to the north and south. South of fault I, the TRB is folded by the Chocolate Drop anticline. To the north of fault I, units are intruded by the Lincoln stock therefore, structural exposure of the anticline is limited. However exposed to the north and east of the stock is a zone of inconsistently oriented structure with stratigraphy that is out of sequence (Plate 1) (Tschanz and Pampeyan, 1970).

New mapping shows the SPFZ is a non-planar segmented fault zone which dips steeply east and places Upper Cambrian units over Mississippian to Pennsylvanian units (Fig. 7, Plate 1). The SPFZ cuts across strike of the Cambrian units on the east and offsets the TRB on the west. Furthermore, south of fault C, the SPFZ splays into multiple strands with three main branches. This fault has three geometric sections based on strike. The entire central section is documented on Plate 1 (Fig. 7), is ~1.4 miles (2.3 km) long, and strikes N-S. The main fault splays to the north and south. At these branch lines/ zones, the main fault bends 30^{o} toward the east in the north and 20^{o} toward the west in the south. These areas of splays form the other two sections. The SPFZ truncates fault C and changes strike at it.

Each branch line/zone is spatially associated with folds (Fold set D, see below) that parallel the splays exposed in the thin-bedded late Paleozoic units, particularly the Pennsylvanian Ely Limestone of the hanging wall. The fault strikes 348^{o} in one measured location on the southeastern splay of the southern segment and 008° along the main fault, and dips 83° and 78° E, respectively (Plate 1). There are minor thrusts which strike 70° to the strike of the SPFZ and outcrop scale folds in two restraining bends along the northern extent of the SPFZ.

Folds

A variety of folds occur in the map area. Folds A, B, and C are macro-scale folds located in the eastern part of the map area, the Chocolate Drop anticline, named here, is a macro-scale fold in the far west of the area, and fold set D is a series of meso-scale folds located near the SPFZ (Fig. 7, Plate 1).

Fold A is exposed in the northern part of the map area (Fig. 7, Plate 1) in the hanging wall of the Lincoln thrust. This fold is an upright, moderately plunging, open syncline. The hinge of fold A has a measured plunge and trend of 38°, 106° (Fig. 10a). Fold A is only exposed in the Ordovician Antelope Valley Limestone.

Fold B, located east of fold A (Fig. 7, Plate 1), is a macro-scale, open, upright, horizontal syncline in the footwall of the Lincoln thrust. The exposed limbs of fold B are composed of Devonian Simonson Dolomite and Guilmette Formation; however the hinge itself is buried by active wash deposits and alluvium. The hinge of fold B has a calculated plunge and trend of 8°, 134° (Fig. 10a). There is a paired anticline to the east cut by two high-angle, normal faults (Fig. 9, Plate 2).

Fold C is a macro-scale syncline in the southern part of the Lincoln thrust plate (Fig. 7, Plate 1). This fold is exposed in the Ordovician Pogonip Group and Eureka Quartzite

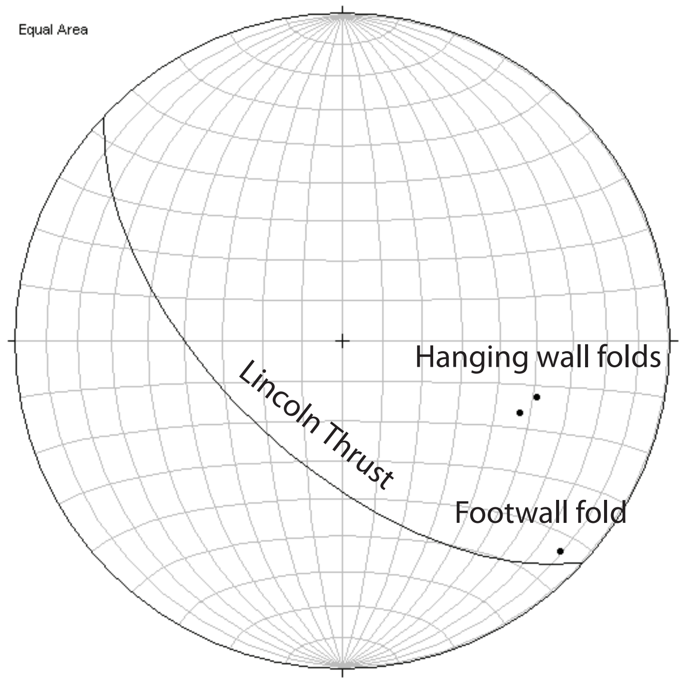

Fig 10a. Stereograph of the Lincoln thrust and associated folds. The great circle represents the Lincoln thrust. The dots show the plunge and trend of folds in the hanging wall and footwall of the Lincoln thrust. Only measured points are shown. Calculated orientations agree with measured values.

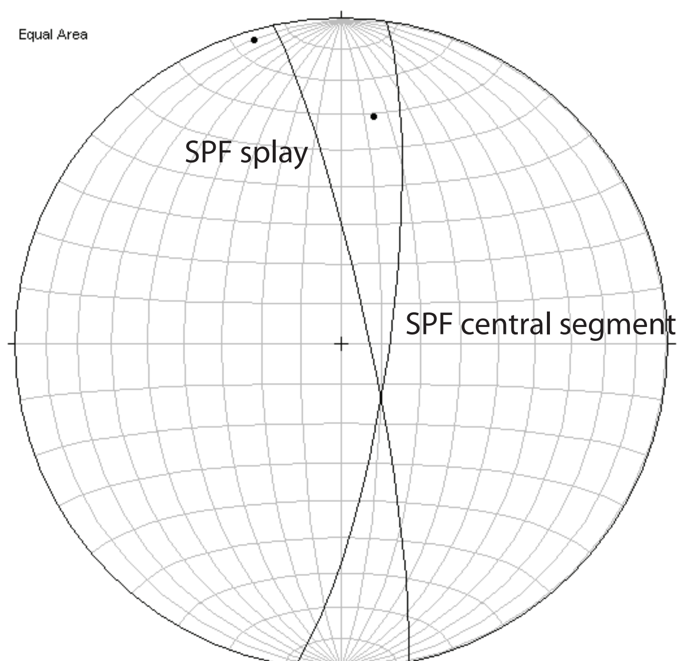

Fig 10b. Stereograph of the SPFZ and related folds. The great circles represent the central segment of the SPFZ and one of the southern splays. The dots show the plunge and trend of folds in fold set D, located in the hanging wall of the central segment and aforementioned splay. Only measured points are shown. Calculated orientations agree with measured values.

in the northeastern portion of the study area. Although limited in exposure, fold C is an upright, NW-trending fold that plunges gently to the SE.

Fold set D is a set of meso-scale, shallow to horizontal, inclined to recumbent anticlines and synclines occurring near the western edge of the map area. These folds are exposed in a few outcrops in the Mississippian Chainman Shale and Pennsylvanian Ely Limestone in the footwall and Upper Cambrian Limestone in the hanging wall of the SPFZ (Fig. 7, Plate 1). The average hinge of fold set D has a plunge and trend of 8°, 339° in the north and 30°, 008° in the south (Fig. 10b).

The Chocolate Drop anticline is a macro-scale, west-vergent, upright anticline exposed in the TRB in the far western part of the map area. Exposed limbs are composed of Mississippian Lower and Upper Joana Limestone, Chainman Shale, Scotty Wash Quartzite, and Pennsylvanian Ely Limestone. Measurements in the field area along with those of Tschanz and Pampeyan (1970) show a plunge and trend of 03°, 003° (Fig. 11). Reconnaissance to the west combined with mapping by Tschanz and Pampeyan (1970) of the map area shows a paired syncline, which makes a fold pair.

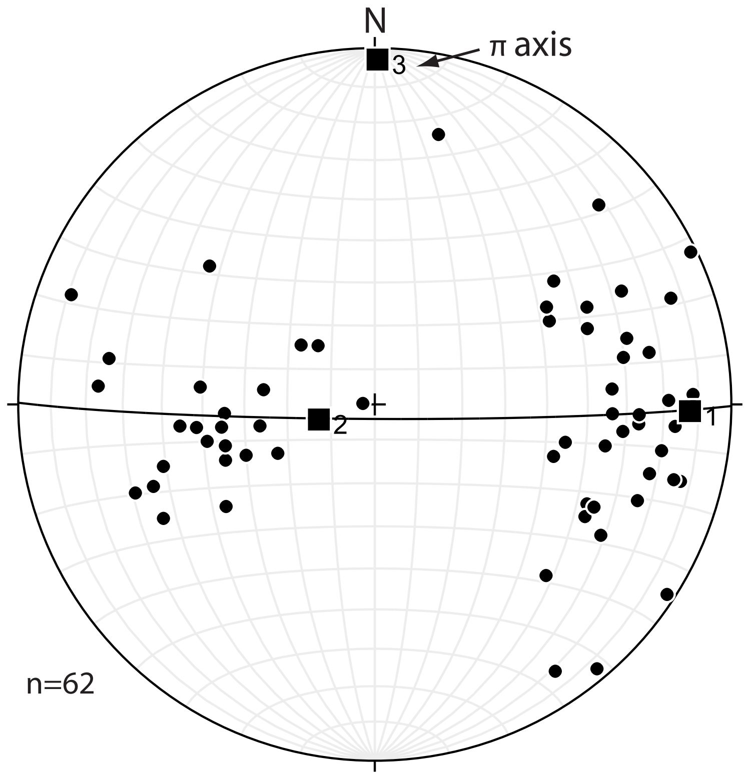

Figure 11. Stereograph of poles to bedding taken from the Chocolate Drop anticline. Data plotted are from new field measurements and data from Tschanz and Pampeyan (1970). Best fit π axis plunge and trend is 03°, 003°.

CHAPTER 5

DISCUSSION

New mapping in the Timpahute Range documents at least four periods of deformation in the area. The deformation includes three contractional events based on cross-cutting relations: the Chocolate Drop anticline (D_1), SPFZ and fold set D (D_2), structures of the CNTB (D_3), and extensional structures including the Tunnel Springs fault (D4). All deformations are younger than the deposition of units from the Antler Overlap sequence (Pennsylvanian Ely Limestone). Contractional deformation pre-dates the 102.9 ± 3.2 Ma emplacement of the Lincoln stock because paleomagnetic data show that the stock lacks the folding/tilting observed in the host rocks (Taylor et al., 2000). Furthermore, although the stock intrudes the TRB/footwall of the SPFZ at the surface, localized contact metamorphism is documented in the upper plates/hanging walls of both the Lincoln thrust and SPFZ, as well as in the TRB. This zone of metamorphism suggests that D_1 – D_3 occurred prior to intrusion. Late stage extensional faults cut Miocene age volcanic rocks in nearby areas (e.g., Taylor et al., 2000).

Contraction

The newly documented Chocolate Drop anticline is interpreted to represent a shortening event isolated to exposures in the TRB. The N-trending hinge of the Chocolate Drop anticline suggests shortening and maximum principal stress directions (σ_1) of E-W when it formed (Fig. 11). The TRB displays the earliest contraction in the map area (D1), which is significant because deformation that occurred before the formation of the Sevier orogenic belt / Central Nevada thrust belt was not known previously in this area.

The geometry and kinematics of the SPFZ (D_2) are clarified by new data. Fold set D is interpreted to be related to the SPFZ (Fig. 10b) and is mostly documented in the thinner bedded units of the footwall of the SPFZ (Plate 1). These N-S trending folds have measured orientations (8^o, 339^o in the central segment and 30^o, 008^o in the southern segment) which are similar to the N- S striking SPFZ (348^o in the central segment and 008^o in the southern segment) (Fig. 7, Plate 1). Fold set D contains recumbant folds that are most likely due to folds that formed in beds previously tilted in the Chocolate Drop anticline. The similarity in trend of the SPFZ and fold set D, the placement of Cambrian units over late Paleozoic units, and steep-east fault dips measured in two locations suggest the SPFZ is a steeply dipping reverse fault. The orientation of the fold hinges and fault strike suggest E-W shortening and that σ_1 is E-W for the SPFZ.

A third contractional event (D_3) occurred in the map area forming this part of the CNTB. This includes the formation of NW-striking thrust faults in the eastern part of the area (Lincoln thrust, fault B, Schofield thrust, and fault H) and NW-trending folds A, B & C (Fig. 7, Plate 1). The orientations of these structures suggest NE-SW shortening and a NE-SW oriented σ_1 (Fig. 10a).

Cross-cutting relations between the Chocolate Drop anticline and SPFZ as well as a difference in measured and calculated structural orientaions of strikes and trends between those structures (N) and structures of the CNTB (NW) (Fig. 7). suggest these structures are unlikely to have formed simultaneously. These distinctly separate orientations suggest kinematic incompatibility. Furthermore, the SPFZ cuts the east limb of the Chocolate Drop anticline. The Chocolate Drop anticline, the SPFZ, and structures of the CNTB are interpreted to represent three separate shortening events because of differing structural and stress orientations, cross-cutting relations, and spatial distribution of deformation.

Relative Timing of Contraction

The SPFZ and the Chocolate Drop anticline have similar orientations. This may suggest that the SPFZ caused the formation of the Chocolate Drop anticline. Alternatively, it is likely the SPFZ may have formed at a similar orientation to earlier folds in the TRB along an already existent axially planar fracture set. Splays of the SPFZ cut across the east limb of the Chocolate Drop anticline (Plate 2) and the smaller folds related to the SPFZ (fold set D) refold the east limb of the anticline (Plate 1). In addition, the SPFZ cuts across the stratigraphy of the Chocolate Drop anticline (across Mississippian Lower Joana Limestone, Chainman Shale, and Scotty Wash Quartzite and Pennsylvanian Ely Limestone) supporting the interpretation that the Chocolate Drop anticline (D_1) pre-dates the SPFZ (D_2).

Based on field relations, the timing of the SPFZ relative to the CNTB could occur in any of three possible ways: (1) the SPFZ occurred first, then the Lincoln thrust rode over top (placing the SPFZ in the lower plate of the Lincoln thrust), and then SPFZ was reactivated during late stage extension as a normal fault; (2) the Lincoln thrust occurred first and the SPFZ occurred second, carrying the CNTB structures in the hanging wall (Fig. 12); or (3) the SPFZ occurred first and the Lincoln thrust occurred second carrying

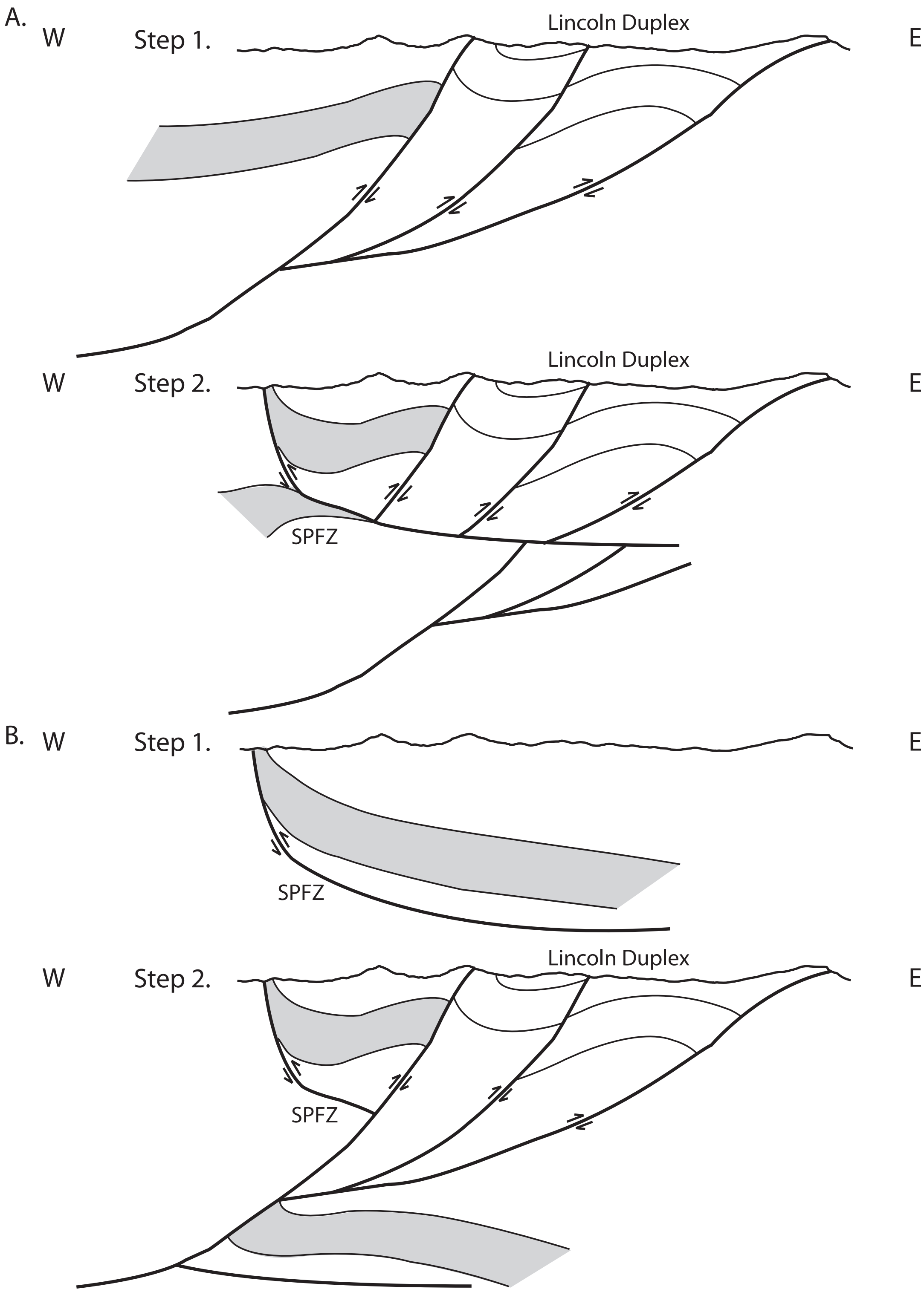

Figure 12. Diagrams for options of the order of faulting between the Schofield Pass fault zone and the Central Nevada thrust belt. A. Lincoln thrust occurred first and SPFZ occurred second, carrying CNTB structures in the hanging wall. B. SPFZ occurred first, Lincoln thrust occurred second and carried the SPFZ passively to the east.

the SPFZ passively to the east in the upper plate (Fig. 12). For each of these possibilities, it is critical to recognize that the facies and thickness of units in the TRB, particularly the Joana Limestone, Chainman Shale, and Guilmette Formation, are different from those exposed in the Lincoln thrust plate and duplex. The TRB contains deeper water deposits, such as more massive exposures of the Scotty Wash Quartzite, mostly silty limestone beds with minor sandstone in the Chainman Shale, Lower Joana exposures containing fewer, smaller, and more variety of marine fossils, and much thinner beds of the Guilmette Formation with almost no sandstone lenses. The exposures of part of the Lower Guilmette Formation, the Alamo breccia, in the TRB are closer to the impact crater than those exposed in Mt. Irish and Monte Mountain (Pinto and Warme, 2008), supporting the interpretation that units of the TRB were deposited farther west than those of the lower plate of the Lincoln thrust. In addition, the units in the Lincoln thrust plate and the Lincoln duplex resemble those in nearby ranges (e.g., Worthington Mountains), indicating that the footwall of the Lincoln thrust should be generally in place with respect to units in those ranges.

The first option suggests that normal- sense motion or reactivation of the SPFZ is large enough to drop the Lincoln thrust sheet and underlying duplex down against the eastern limb of the Chocolate Drop anticline prior to instruction of the Lincoln stock at 102.9 Ma. In this case, the footwall rocks to the Lincoln duplex would have facies similar to those in the TRB / footwall of the SPFZ, which contradicts observationsthe facies and unit thicknesses of rocks in the TRB are different from those of the Lincoln duplex footwall. In addition, the Lincoln thrust may have carried the upper continuation of the SPFZ eastward. No known west-vergent thrust fault with appropriate offset is known to the east, suggesting this option is not possible.

The second option (Lincoln thrust first) also requires that the formations in the TRB are similar to the Lincoln thrust plate if the SPFZ has relatively small offset. If the SPFZ offset is relatively large or moderate, then the TRB rocks should match those in the Lincoln duplex or units below the duplex. Again, this is not the situation (Fig. 12).

The third option seems most likely (Fig. 12). In this scenario, the SPFZ occurred first, cutting through the eastern limb of the Chocolate Drop anticline and placing the early Paleozoic units up against the rocks of the TRB. Then the Lincoln thrust moved up a ramp into the relatively shallow water rocks and carried the SPFZ passively up the ramp. The rocks immediately east of the SPFZ are all part of the Lincoln thrust plate. Also, during or shortly after motion on the Lincoln thrust the SPFZ may have been reactivated as a back thrust and the Schofield thrust moved. The uplift of the TRB along a ramp in the Lincoln and Schofield thrusts is consistent with the relatively high level of the block relatively to the Paleogene unconformity (c.f., Long, 2012).

Lincoln Duplex

The Lincoln duplex (D_3) is a major contractional structure of the CNTB (Taylor et al., 2000). Orientation, geometry, and timing relative to other structures suggest that the Lincoln thrust, fault B, Schofield thrust, and fault H are all associated with each other. The duplex is roofed by the Lincoln thrust, which places Cambrian and Ordovician units over Devonian and Mississippian units (Taylor et al., 2000; this paper). The Schofield thrust makes a logical floor thrust of the Lincoln duplex. The Schofield thrust places

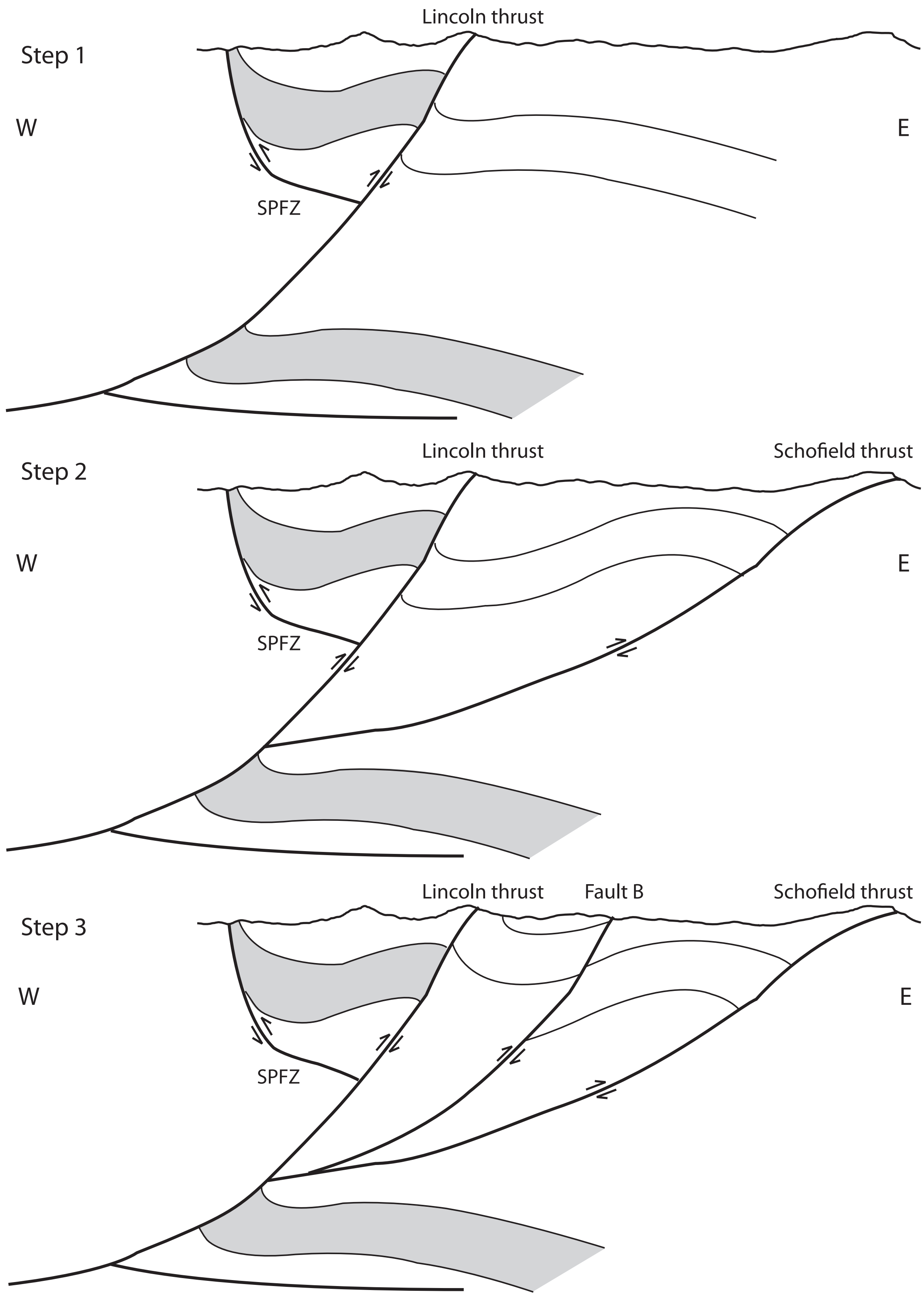

Figure 13. The Lincoln duplex. Steps in the formation of an out-of-sequence hinterland-dipping duplex.

Devonian Guilmette Formation over an overturned syncline exposed in Mississippian units, as is typical in the footwall of thrust faults (Plate 2). This syncline could be a drag fold from the thrust fault or a part of an anticline-syncline pair from a fault propagation fold. Given calculated orientation, geometry, and offset, fault H is interpreted as a splay off the Schofield thrust (Plate 2). A reconstruction of the duplex (Fig. 13) shows the Schofield thrust is the farthest east of the thrust faults associated with the duplex (Fig. 7, Plate 1) and displays limited stratigraphic separation, common for a floor thrust. Similarities in stratigraphic offset and orientation, along-strike proximity, and observed exposures (W.J. Taylor, personal correspondence) suggests the Monte Mountain thrust, located to the southeast, may be a southern continuation of the Schofield thrust. This interpretation is further supported by the amount of left-lateral offset documented along the Tunnel Springs fault.

Due to the orientation of the units and thrusts within the duplex, the Lincoln duplex is interpreted to have formed by a modified variation of a hinterland-dipping duplex (Plate 2) (Boyer and Elliot, 1982). The model of a hinterland-dipping duplex suggests (1) uniform units within each horse which should roughly parallel the subsidiary faults and (2) faults that young toward the foreland (Fig. 6) (e.g., Boyer and Elliot, 1982). These relations would manifest themselves as a repetition of the same stratigraphic sequence of units with the same orientation, which is not documented in this duplex. Furthermore, beds of individual horses should trace out an elongated fold pair, which is lacking in each horse of the Lincoln duplex. A modification to the traditional hinterland-dipping duplex is needed to explain the mapped unit thicknesses, bedding and fault orientations, and folds which differ from the model. If the Lincoln thrust developed as a roof thrust followed by the Schofield thrust as a floor thrust, the developed horse would mirror the orientation of bounding faults, and contain an elongated anticline-syncline fold pair (Fig. 13). If fault B, near the center of the duplex, occurred third, it would cut through the existing fold pair. The later fault B would then cut through the folds. Based on the cut-off lines and projected branch point of fault B, the syncline remained on the side of the roof thrust and the anticline remained with the floor thrust. Also, based on stratigraphic separation, the horses in this duplex have unequal length and offset (Fig. 13, Plate 2). An out-of-sequence thrust could generate horses with those physical characteristics (Fig. 13, Plate 2).

Fault I

Fault I appears to cut across the TRB (Fig. 7, Plate 1). In the TRB to the north and south of fault I, the structures have similar geometries and orientations, but are not continuous across it. Mapping out the structures north of fault I is complicated by the Lincoln stock and local metamorphism of units. Fault I may have been a pre-existing structure that accommodated different amounts or styles of contraction north and south of the fault. If fault I is younger than the Chocolate Drop anticline, then the anticline would be simply offset and more uniformity should be seen in the structures to the north and south of the fault. The differences could be due to younger structural overprinting. However, a more likely interpretation is that fault I may accommodate the differences between the zone of the TRB intruded by the Lincoln stock and the Chocolate Drop anticline, and thus, is a relatively young structure.

Extension and Reactivation

D_4 includes NW-striking normal faults D, E, F, and G as well as the left-lateral Tunnel Springs fault (Fig. 7). It is likely that all of the documented extension in the area occurred synchronously because the faults all share the same northwest strikes. However, no data known at this time indicate directly whether this extension is Cretaceous or Tertiary in age.

Normal faults F and G are not continuous across the Tunnel Springs fault nor do they offset it (Fig. 7, Plate 1). Because these normal faults terminate at the Tunnel Springs fault, slip along these normal faults must transfer onto the Tunnel Springs fault. Fault E may truncate the Tunnel Springs fault. However, the magnitude of extension differs along fault E north and south of the Tunnel Springs fault so a more likely interpretation is that the Tunnel Springs fault dies out in the graben between faults D and E (Fig. 7). Reconnaissance to the east and mapping of an unnamed strike-slip fault by Tschanz and Pampeyan (1970) and Sandru and Taylor (2003) indicates that the fault continues farther to the east. The unnamed fault cuts Tertiary volcanic rocks, which suggests that extension in the Timpahute Range is Cenozoic in age.

Reactivation of the SPFZ as a right-lateral strike-slip fault is documented by a series of restraining bends with associated contractional structures such as meso scale folds and a small pop-up block (Plate 1). This reactivation must be older than the intrusion of the Lincoln stock, because units on both sides of the SPFZ are metamorphosed.

The southern central splay of the SPFZ is interpreted to also be reactivated as a normal fault. This reactivation is documented by the placement of Pennsylvanian Ely

Limestone atop Mississippian Lower Joana Limestone. However, fold set D is located in the footwall of this splay suggesting a reverse fault. So, reactivation is necessary to explain both attributes.

CHAPTER 6

REGIONAL INTERPRETATIONS

West-Vergent Structures

Correlating west-vergent structures of the Timpahute Range is problematical given their location and orientation combined with the Pennsylvanian to 102.9 Ma (early Cretaceous) age brackets. West-vergent structures, which are relatively rare, are documented in Death Valley (White Top Mountain backfold/fold pair and Winter's Peak anticline of Snow and Wernicke, 1989; c.f., Renik and Christie-Blick, 2012) but may have timing issues because to the south they are thought to be late Cretaceous in age. Two west-vergent structures are documented to the south in the Nevada Test site: the Pintwater anticline (Guth, 1981; Guth, 1990; Caskey and Schweickert, 1992) and the CP thrust (Fig. 2, Table 1) (Caskey and Schweickert, 1992; Cole and Cashman, 1999). Structures of Permian age are documented in northern Nevada (Cashman et al., 2011) and to the west and northwest as part of the Permo-Triassic Luning-Fencemaker belt (Wyld et al., 2001; Wyld, 2002), but these structures are east vergent. Minor west vergent thrusts were mapped in the northwestern Quinn Canyon Range (Bartley et al., 1988) but have much smaller offset, placing Upper and Middle Cambrian rocks over Middle Cambrian. West-vergent structures in northern Nevada are middle Pennsylvanian (Cashman et al., 2011) and post-Sonoma orogeny (Villa, 2007) and may possibly correlate.

Tempiute Ridge Block/ Chocolate Drop Anticline

Given the size of the Chocolate Drop anticline and paired syncline, it seems likely that it continues along strike. Northern Nevada deformation (Villa, 2007; Cashman et al.,

2011) could correlate based on vergence and timing. W- to SW-vergent folds are documented in northern Nevada between the middle Atokan and late Missourian (Villa, 2007; Cashman et al., 2011), however these folds are tight to close, moderately to steeply inclined and developed by northeast-southwest shortening. These structures could only correlate to the Chocolate Drop anticline if the folding began immediately following the deposition of the Pennsylvanian Ely Limestone but would not be likely due to differing geometries and stress directions. A preferable correlation would be to the west-vergent D_5 deformation (Villa, 2007) of Edna Mountain, which is defined by the F_5 folds and Edna Mountain syncline (Cashman et al., 2011). These open, map-scale folds show a plunge and trend of 04^o, 356^o which is similar to the Chocolate Drop anticline (open, macro-scale, with a plunge and trend of 03,000). The west-vergent folds at Edna Mountain fold the Golconda allochthon which suggests folding is post Sonoma orogeny (Villa, 2007), late Permian to early Triassic (Dickinson, 2006). To the south, the CP thrust (Caskey and Schweickert, 1992; Cole and Cashman, 1999; Long, 2012) may potentially be correlative, due to timing and vergence, but may better fit elsewhere, possibly with the SPFZ. Structures of similar timing may be more likely to be correlative if the Chocolate Drop anticline is only locally west-vergent rather than a regional trend. However, no data is available with which to determine that at this time.

Schofield Pass Fault Zone

The SPFZ is a major west-vergent thrust with multiple strands locally. In nearby ranges to the north, there are no known west vergent structures of this magnitude (only some of lesser magnitude, see above; Table 1) (Bartley et al., 1988), suggesting either the

SPFZ is buried under the Sand Spring Valley or dies out. Two potentially correlative structures lie to the south: the Pintwater anticline and the CP thrust (Fig. 2, Table 1) (Guth, 1981; Guth, 1990; Caskey and Schweickert, 1992; Cole and Cashman, 1999). The horizontal map distance between the Mt. Irish thrust and SPFZ is significantly greater than that between the Gass Peak thrust and the Pintwater anticline (Fig. 2). Without a known significant difference in the magnitudes of extension, this relation suggests that the Pintwater anticline and the SPFZ do not correlate to each other. A preferable alternative is a correlation of the CP thrust to the SPFZ. The two west-vergent systems have similarities in stratigraphic separation (Table 1). The CP thrust does not continue exactly along strike of the SPFZ presenting a deficiency in spatial correlation, however, left-lateral offset along Cenozoic faults to the south of the Timpahute Range may accommodate this difference. Given the similarities in orientation between the Chocolate Drop anticline and SPFZ and likelyhood the SPFZ formed in an area of pre-existing weakness of the Chocolate Drop anticline, it is plausible that both the west-vergent structures of the Timaphute Range may correlate to structures within a southeastward zone of structures which are related to the CP thrust (Panama thrust, Titus Canyon syncline, etc.) (Snow and Wernicke, 1989; Caskey and Schweickert, 1992).

A map of exposures of the Sevier hinterland under the Paleogene unconformity (Long, 2012) suggest the west-vergent structures of the TRB (including the Chocolate Drop anticline and SPFZ) are not continuous to the north and south. This could suggest the continuation of the block may have been eroded under the unconformity or lies buried under basin fill. A more likely alternative is that the relation further supports the interpretation that the TRB and associated structures (Chocolate Drop anticline and SPFZ) originated farther to the west and were carried eastward relative to the craton. Furthermore, the map implies that southward continuation of the pre-existing west-vergent structures were cut by the Lincoln-Spotted Range thrust (CNTB) (Long, 2012) supporting the relative timing of deformation in the Timpahute Range and suggesting correlative structures may be found more to the east.

Lincoln Thrust, Schofield Thrust and Lincoln Duplex

To the north, the Lincoln thrust has been correlated to the Freiberg-Rimrock thrusts (Fig. 2) (Bartley and Gleason, 1990; Taylor et al., 2000). These three faults are correlated by similarities in stratigraphic separation and Pogonip Group facies in the hanging wall (Table 1).

No evidence suggests that the Lincoln duplex dies out toward the south. Individually, however, thrusts of the duplex may rejoin, consequently at least some thrusts may correlate to the south. Two east-vergent thrusts are exposed between the west-vergent CP thrust and the Gass Peak thrust: the Pintwater thrust and the Spotted Range thrust. The Pintwater thrust juxtaposes Cambrian Bonanza King Formation with rocks as young as the Devonian Sevy Dolomite making correlation to this structure a possibility (Fig. 2, Table 1).

The Spotted Range thrust also shares a similar amount of stratigraphic separation with the Lincoln thrust (Fig. 2, Table 1). The mapped strikes differ between the N-striking Spotted Range thrust and the NW-striking Lincoln thrust, however variations in the amounts of Tertiary extension to the north and south or a primary bend in the thrust(s) may account for this difference. This suggestion is corroborated by Long's (2012) Paleogene paleogeologic map construction, which supports the correlation of the two thrusts by Taylor et al. (2000). Taylor et al. (2000) cited complications correlating the two structures due to overturned, tight to isoclinal folds present in the footwall of the Spotted Range thrust (Barnes et al., 1982). However, these folds may be related to the newly mapped overturned fold below the Lincoln duplex/Schofield thrust (Figs. 7 and 9, Plates 1 and 2). Consequently, correlation of the Lincoln thrust to the Spotted Range thrust appears reasonable.

Tunnel Springs Fault

The Tunnel Springs fault correlates to an unnamed strike-slip fault of Tschanz and Pampeyan (1970) (Fig. 2 Regional) eastward along strike and into the Mt. Irish Range (Sandru and Taylor, 2003). This major strike-slip fault relates spatially to a belt of E- to NE-striking strike-slip faults known as the Timpahute Lineament which lies along a broader zone of strike slip across the region, including the Pahranagat Shear Zone and faults of the Hiko Range (Jayko, 1990; Tingley, 1991; Taylor and Switzer, 2001).

CHAPTER 7

CONCLUSIONS

Identification and description of structures in the Timpahute Range clearly defined structural geometries and cross-cutting relations. Furthermore, timing of these CNTB and older folds and faults, allows possible correlation with other structures in the region. Correlation of older structures, the Chocolate Drop anticline and SPFZ, is less precise than that of the CNTB structures. All of the contractional structures were active between deposition of the Pennsylvanian Ely limestone and emplacement of the 102.9 ± 3.2 Ma Lincoln stock.

The earliest deformation in the Timpahute Range is the west-vergent Chocolate Drop anticline of the TRB. This deformation is older than the SPFZ and the CNTB. This early contraction is significant because deformation between the Antler and Sevier in age was unknown the area. Confident correlation of this anticline northward is made uncertain by the large distance to identified W-vergent structures, but the D_5 folds documented at Edna Mountain (Cashman et al., 2011) are a reasonable possibility. Southward, the Chocolate Drop anticline may correlate to the CP thrust or may be cut off by the Lincoln thrust or its equivalent.

The SPFZ is a non-planar W-vergent reverse fault that places Upper Cambrian units of the Lincoln thrust plate over Mississippian to Pennsylvanian units of the Chocolate Drop anticline. The preferred interpretation of the timing of the SPFZ is that the Lincoln thrust cut the SPFZ which carried it passively to the east and up a ramp.

Given the similarities between the Chocolate Drop anticline and SPFZ, the SPFZ may have formed along an pre-existing weakness of an axially planar fracture set. Therefore, it is plausible these structures may both or either correlate southward to the CP thrust and/or a zone of related west-vergent structures including the Panama thrust and Titus Canyon syncline or be cut off by the Lincoln thrust. Furthermore, these structures pre-date the occurance of the CNTB and may complete a belt of pre-Sevier aged deformation from Death Valley to nothern Nevada.

The Lincoln thrust roofs the Lincoln duplex, which is the main CNTB structure in the area. Based on the juxtaposition of Ordovician or Cambrian over Devonian – Mississippian units and spatial position, the Lincoln thrust appears to correlate southward with the Spotted Range thrust while to the north the thrust and duplex correlate to the Lincoln duplex of the Worthington Mountains (Taylor et al., 2000) and then continue northward to the Frieberg-Rimrock thrusts (Bartley and Gleason, 1980). The Lincoln duplex is an out-of-sequence hinterland-dipping duplex; this interpretation differs from previously proposed end-member models of duplex development.

A major left-lateral strike-slip fault (Tunnel Springs fault) formed during Cenozoic extension. The Tunnel Springs fault offsets units and older structures in multiple mountain ranges to the east. In the Timpahute Range, the Tunnel Springs fault separates and displaces the Schofield thrust from its southward continuation, the Monte Mountain thrust. Furthermore, mapping of faults in the area suggests transfer of extension from normal faults to the Tunnel Springs fault. The Tunnel Springs fault appears to be related to the Timpahute Lineament, a series of E-W to NE-SW striking strike-slip faults that cut across the region.

APPENDIX A: TABLE 1 REGIONAL STRUCTURES

Structure	Vergence	Strike	Offset	Age	Comments	Reference
Southern						
Belted Range thrust	ESE	N	Pennsylvanian over Silurian/Devonian over Mississippian	Predates White Top Stock (228±2Ma)	Correlated to Last Chance thrust	Caskey and Schweickert, 1992; Cole and Cashman, 1999
CP thrust	W	NNE	late Precambrian/ Cambrian over Pennsylvanian/ Permian	Between Belted Range thrust and Climax Stock (93 Ma)		Caskey and Schweickert, 1992; Cole and Cashman, 1999
Spotted Range thrust	E	N	Cambrian over Devonian/ Mississippian	Same as Belted Range thrust?	Possibly correlated to Belted Range. Overturned isoclinal folds.	Caskey and Schweickert, 1992; Cole and Cashman, 1999
Pintwater thrust	E	N	Cambrian over Silurian/Devonian		Offset obscured by tertiary overprinting	Guth, 1990; Caskey and Schweickert, 1992
Pintwater anticline	W	N	Devonian/ Mississippian	Sevier?	Formed over east-vergent duplex in subsurface	Caskey and Schweickert, 1992; Cole and Cashman, 1999

APPENDIX A: TABLE 1 REGIONAL STRUCTURES

Structure	Vergence	Strike	Offset	Age	Comments	Reference
Central						
Chocolate Drop anticline	W	N	Mississippian/ Pennsylvanian	Predates Lincoln Stock (109Ma)	Earliest contractional deformation in Timpahute Range	This document
Schofield Pass fault zone	W	N	Cambrian over Devonian/ Pennsylvanian	Predates Lincoln Stock (109Ma)		Taylor et al., 2000, This document
Lincoln thrust	NE	NW	Ordovician over Devonian/ Mississippian	Predates Lincoln Stock (109Ma)	Footwall (FW) ramp	Taylor et al., 2000, This document
Fault B	NE	NW	Devonian over Mississippian		Interior thrust of Lincoln duplex	This document
Schofield thrust	NE	NW	Devonian over Mississippian		May be bottom of Lincoln duplex	Taylor et al., 2000, This document

APPENDIX A: TABLE 1 REGIONAL STRUCTURES

Structure	Vergence	Strike	Offset	Age	Comments	Reference
Fault H	NE	NW	Mississippian over younger Mississippian		Faulted overturned syncline	This document
Monte Mountain thrust	E	N	Devonian over Mississippian		Correlates to Schofield thrust	Taylor et al., 2000, This document
Mt. Irish thrust	E	N	Ordovician over Devonian		Correlated to Gass Peak thrust	Taylor et al., 2000; Bidgoli, 2005
Timber Mountain anticline	E	NE		Mesozoic	Overturned anticline	Fryxell, 1988
Northern						
Rimrock thrust	E	NNE	Ordovician over Devonian		In FW of Sawmill thrust, open upright anticline in HW (fault propagation fold)	Bartley and Gleason, 1990

APPENDIX A: TABLE 1 REGIONAL STRUCTURES

Structure	Vergence	Strike	Offset	Age	Comments	Reference
Sawmill thrust	E	NW	Ordovician over Devonian/ Cambrian over Silurian-Devonian		Fault bend anticline in hanging wall (HW) at top of ramp	Bartley and Gleason, 1990
Frieberg thrust	E	N	Ordovician over Ordovician/ Ordovician over Devonian			DuBray, 1968; Martin, 1987
Golden Gate thrust	E	N	Ordovician over Mississippian	Sever, early Cretaceous	Correlated to Mount Irish thrust	Armstrong and Bartley, 1993

APPENDIX B: UNIT DESCRIPTIONS

(Quaternary) Active washes, inset into older alluvium, clasts derived from local sources.

(Quaternary) Older alluvium and colluvium, silt-sized to small boulders on slopes, clasts derived from local sources.

(Tertiary) Volcanic tuff. Rhyolitic to dacitic, altered welded tuff, lithic fragments up to 0.75 cm, red-purple in color, contains feldspar and quartz phenocrysts.

(Cretaceous) Lincoln stock. Quartz monzonite, equigranular, 102.9 ± 3.2 Ma.

(Pennsylvanian) Ely Limestone. Blue-grey to blue-tan weathering, blue to blue-grey fresh, fine grained micrite, some crystalline, local chert stringers, interbedded sandstone, tan to light brown-grey weathering, brown to grey-blue fresh; contains brachiopods, crinoids, mollusks, and fusulinids, abundant in some beds; locally metamorphosed by Lincoln stock. Thick, massive beds, slope former. Entirely fault bound in field area. Unit is at least 1500 ft (457 m) thick (Tschanz and Pampeyan, 1970).

(Mississippian) Scotty Wash Quartzite. Weathers brown, various shades of brown fresh, fine-medium grained silica cemented sandstone (orthoquartzite); medium-thick bedded in the TRB, local ripple marks, recrystallized near Lincoln stock. Massive cliff former or talus slopes. Partially fault bound. Regional thickness of 500 ft (152 m) (Tschanz and Pampeyan, 1970).

(Mississippian) Chainman Shale. Light-dark grey to tan weathered, black-grey fresh, shale with interbedded calcareous shale in the footwall of the Lincoln thrust, silty shale/siltstone with some sandstone lenses in the TRB. Highly eroded slope and valley former. Unit is approximately 300 ft (91 m) thick.

(Mississippian) Upper Joana Limestone. Light grey to tan weathered, light grey to dark grey fresh, fine to medium grained micrite, local chert; some crinoids, only erosional surfaces in field area. Thin to medium bedded, small cliffs and ledges. Regional thickness is approximately 500 ft (152 m), estimated from the unnamed Mississippian limestone of Tschanz and Pampeyan (1970).

(Mississippian) Lower Joana Limestone. Light blue to grey weathered, very blue to dark grey fresh, coarse grained micrite, chert stringers; eastern exposures are abundant in large (1-2cm) crinoid stems, the TRB contains mollusks, bryozoans, and fewer and smaller crinoids. Many massive beds, cliff former. Regional thickness of unit is approximately 500 ft (152 m) thick, estimated from the unnamed Mississippian limestone of Tschanz and Pampeyan (1970).

APPENDIX B: UNIT DESCRIPTIONS

(Devonian) Guilmette Formation. Light grey weathered, medium to dark grey fresh, fine grain micrite, locally dolomitic, silica cemented sandstone/orthoquartzite lens, grey to tan weathered, light to dark grey fresh. Medium to thick beds in the footwall of the Lincoln thrust. Much thinner beds with almost no sandstone are exposed in the TRB. Massive cliff and slope former. Mostly fault bound in field area. Unit is 2200 ft (671 m) thick (Tschanz and Pampeyan, 1970).

(Devonian) Simonson Dolomite. Brown to brown-grey weathered, dark blue to brown fresh, coarsely crystalline, local chert lenses. Cliff former. Exposure is of strata near middle of unit. Regional thickness of 1600 ft (488 m) thick (Tschanz and Pampeyan, 1970).

(Devonian) Sevy Dolomite. Not exposed in field area. Regionally 600 ft (183 m) thick (Tschanz and Pampeyan, 1970).

(Silurian) Laketown Dolomite. Not exposed in field area. Regionally 410 ft (125 m) thick (Tschanz and Pampeyan, 1970).

(Ordovician) Fish Haven Dolomite. Not exposed in field area. Regionally 220 ft (67 m) thick (Tschanz and Pampeyan, 1970).

APPENDIX B: UNIT DESCRIPTIONS

(Ordovician) Eureka Quartzite. Grey to tan weathered, white to pink fresh, silica cemented sandstone (orthoquartzite); fine to medium grained, sugary. Large ledge former or boulder (up to 3 meters) covered slopes. Unit is approximately 800 ft (244 m) thick.

(Ordovician) Pogonip Group:

- Antelope Valley Limestone. Tan to yellow-tan weathered, grey to brown fresh, medium grained limestone; fossil hash in west, receptaculites in east; thin to medium beds. Valley and small cliff former in top of section. Contacts are predominantly faulted in field area. At least 620 ft (189 m) thick in field area.
- Ninemile Formation. Tan weathered to medium grey fresh, silty shale, locally calcareous, thin sandy limestone beds. Valley former. Limited exposure, mostly faulted out in field area. Approximately 830 ft (253 m) thick in region, formation thickness estimated from regional thickness of the Group from Tschanz and Pampeyan (1970).
- Goodwin Limestone. Light grey weathered to dark grey fresh, fine grained micrite, chert nodules at base of unit; girvanella. Thick, massive beds lower in unit, cliff former. Approximately 1450 ft (442 m) thick calculated in map area.

(Cambrian) Upper Upper Cambrian. Light grey weathered to medium grey fresh limestone, fine to medium grained, inter-layered brown chert (approximately 10-14cm layers), metamorphosed locally by Lincoln stock. Slope and cliff former. Approximately 600 ft (183 m) thick calculated in map area.

(Cambrian) Lower Upper Cambrian. Light and dark grey weathered or fresh, dominantly marble, some fine grained limestone to the south. Slope former. At least 1600 ft (488 m) thick exposed in field area.

APPENDIX C: ZIRCON DATA

Name	Age (Ma)											Correlation				
	$^{206}Pb/^{238}U$	1 s.e.	$^{207}Pb/^{235}U$	1 s.e.	% Radiogenic ^{206}Pb	$^{206}Pb^{*}/^{238}U$	1 s.e.	$^{207}Pb^{*}/^{235}U$	1 s.e.	$^{207}Pb^{*}/^{206}Pb^{*}$	1 s.e.	of Concordia Ellipses	$^{204}Pb/^{206}Pb$	1 s.e.	Th/ U	U ppm
2010_07_27July\ TR_AR_01int.ais	103	4	49	4	96.7	0.0161	0.0006	0.050	0.004	0.02234	0.00176	0.48	0.00011	0.00004	0.167	4200
2010_07_27July\ TR_AR_01r.ais	98	4	98	4	100.0	0.0154	0.0006	0.102	0.004	0.04781	0.00112	0.83	0.00018	0.00007	0.071	1900
2010_07_27July\ TR_AR_01r4.ais	108	4	108	4	99.8	0.0169	0.0006	0.112	0.004	0.04814	0.000529	0.96	0.00022	0.00005	0.071	7100
2010_07_27July\ TR_AR_01rr.ais	174	8	213	10	98.8	0.0274	0.0013	0.234	0.012	0.06181	0.00103	0.94	0.00045	0.00010	0.074	1800
2010_07_27July\ TR_AR_01rrr.ais	100	3	100	4	99.1	0.0157	0.0005	0.104	0.005	0.04792	0.00137	0.76	0.00056	0.00010	0.108	3000
2010_07_27July\ TR_AR_2int.ais	125	4	101	5	97.0	0.0196	0.0006	0.105	0.005	0.03897	0.00158	0.61	0.00035	0.00011	0.046	1000
2010_07_27July\ TR_AR_2r.ais	104	4	104	4	99.9	0.0163	0.0006	0.107	0.004	0.04785	0.000676	0.94	0.00019	0.00005	0.010	4200
2010_07_27July\ TR_AR_2r3.ais	105	3	105	3	99.4	0.0164	0.0005	0.109	0.004	0.04832	0.000436	0.96	0.00035	0.00005	0.014	7700
2010_07_27July\ TR_AR_2rr.ais	136	7	106	6	97.7	0.0213	0.0011	0.110	0.007	0.03744	0.0012	0.86	0.00018	0.00010	0.027	2400

$^{206}Pb/^{204}Pb$ common is 18.86
$^{207}Pb/^{204}Pb$ common is 15.62
$^{208}Pb/^{204}Pb$ common is 38.34
Th/U relative sensitivity factor is 1.102
$U/^{94}Zr_2O$ relative sensitivity factor is 0.00391

APPENDIX D: FIELD DATA AND AREA STOP/MEASUREMENT LOCATION MAP

Stop number	Feature	Map Unit	Az◦/ Trend◦	Dip◦/ Plunge◦	Dip D	Comments
1	bedding	lPe	344	52	NE	
2	bedding	lPe	352	36	NE	
3	bedding	lPe	339	32	NE	
4	bedding	lPe	357	35	NE	
5	bedding	Opg	305	21	NE	
6	bedding	Opg	332	45	NE	
7	bedding	Opg	349	40	NE	
8	bedding	Opg	310	60	NE	
9	bedding	Opg	281	32	NE	
10	bedding	Opa	298	12	NE	
11	bedding	Opa	312	21	NE	
12	bedding	lPe	290	20	NE	
13	bedding	lPe	340	37	NE	
14	bedding	lPe	334	25	NE	
15	bedding	lPe	350	27	NE	
16	bedding	lPe	345	36	NE	
17	bedding	lPe	353	42	NE	
18	bedding	lPe	8	26	NE	
19	bedding	lPe	6	41	NE	
20	fault	lPe	39	22	NE	SPFZ lPe/Єl
21	bedding	Opg	283	25	SE	
22	bedding	Opg	290	26	NE	
23	bedding	Opg	333	12	NE	
24	bedding	Єu	245	19	NW	
25	bedding	Єu	295	13	NE	
26	bedding	Єu	316	10	NE	
27	bedding	Opg	315	22	NE	
28	bedding	Opg	270	30	NE	
29	bedding	Opg	275	20	NE	
30	bedding	Opg	290	40	NE	

APPENDIX D: FIELD DATA AND AREA
STOP/MEASUREMENT LOCATION MAP

Stop number	Feature	Map Unit	Az◦/ Trend◦	Dip◦/ Plunge◦	Dip D	Comments
31	bedding	Opg	285	30	NE	
32	bedding	Opg	284	52	NE	
33	bedding	Opg	274	50	NE	
34	bedding	Єu	300	49	NE	
35	bedding	lPe	330	28	NE	
36	fault	lPe	70	85	SE	SPFZ lPe/lPe left splay
37	bedding	Mjl	20	80	SE	
38	fault	Mjl	294	63	NE	splay?
39	fault	Mjl	40	76	SE	splay?
40	bedding	Mjl	10	65	SE	
41	fault	Mjl	50	28	SE	
42	fault	Mjl	35	85	SE	SPFZ Msw/Mjl left splay
43	fault	Mjl	0	73	E	SPFZ Msw/Mjl left splay
44	bedding	lPe	332	57	NE	
45	bedding	lPe	340	56	NE	
46	fold	Єl	344	3		meso-scale, recumbent
47	bedding	Mjl	285	56	NE	
48	bedding	Єu	325	9	NE	
49	bedding	Єl	20	31	SE	
50	bedding	Mc	46	19	SE	
51	bedding	Mc	4	67	E	
52	bedding	Mc	340	61	NE	
53	bedding	Mc	40	51	SE	
54	bedding	Єl	290	54	SW	
55a	bedding	Mc	300	61	SW	
55b	fault		10	82	E	SPFZ main branch
55c	fold	Mc	339	8		
56a	fold	lPe	30	8		
56b	fault		348	83	E	SPFZ southern central splay
57a	bedding	Єu	312	31	NE	

APPENDIX D: FIELD DATA AND AREA STOP/MEASUREMENT LOCATION MAP

Stop number	Feature	Map Unit	Az∘/ Trend∘	Dip∘/ Plunge∘	Dip D	Comments
57b	fault		8	78	E	SPFZ main branch
58	bedding	Єl	27	37	SE	
59	bedding	Єl	4	12	SE	
60	bedding	Єl	9	15	SE	
61	bedding	Єl	335	31	NE	
62	bedding	Mc	40	32	SE	
63	bedding	Mc	290	37	SW	
64	bedding	Mc	44	27	SE	
65	fault	Mjl	72	83	SE	pop-up block
66	fault	Mjl	65	50	SE	pop-up block
67	bedding	Єl	320	58	SE	
68	bedding	Єl	320	71	SE	
69	bedding	Єl	335	38	SE	
70	bedding	Єu	345	35	SE	
71	fault	Єl	10	76	E	SPFZ main branch
72	bedding	Mjl	310	83	NE	
73	bedding	Mc	330	76	NE	
74	bedding	Mc	322	86	NE	
75	bedding	Mjl	316	46	E	
76	bedding	Mc	80	30	E	
77	bedding	Mju	310	40	NE	
78	bedding	Mjl	55	35	NW	
79	bedding	Dg	0	40	E	
80	bedding	Mju	4	69	NW	
81	bedding	Mju	313	54	SW	
82	bedding	Mjl	76	40	SE	
83	bedding	Mjl	280	60	NE	
84	bedding	Mjl	287	77	NE	
85	bedding	Mc	335	35	NE	
86	bedding	Єu	134	56	NE	

APPENDIX D: FIELD DATA AND AREA
STOP/MEASUREMENT LOCATION MAP

Stop number	Feature	Map Unit	Az◦/ Trend◦	Dip◦/ Plunge◦	Dip D	Comments
87	bedding	Єu	330	55	NE	
88	bedding	Єu	330	54	NE	
89	bedding	Opg	355	40	NE	
90	bedding	Opg	325	54	NE	
91	bedding	Opg	335	69	NE	
92	bedding	Opg	315	52	NE	
93	bedding	Opg	324	50	NE	
94	bedding	Opa	320	67	NE	
95	bedding	Opg	310	60	NE	
96	bedding	Opg	317	50	NE	
97	bedding	Єu	336	44	NE	
98	bedding	Єl	355	40	NE	
99	bedding	Єl	310	24	NE	
100	bedding	Єl	350	26	NE	
101	bedding	Єl	5	30	SE	
102	bedding	Єu	315	15	NE	
103	bedding	Єu	330	58	NE	
104	bedding	Єu	60	78	SE	
105	bedding	Opg	295	31	NE	
106	bedding	Opg	282	42	NE	
107	bedding	Opn	320	31	NE	
108	bedding	Opg	318	41	NE	
109	bedding	Mjl	335	51	NE	
110	bedding	Mju	63	35	SE	
112	bedding	Mju	340	34	SW	
113	bedding	Mju	335	42	SW	
114	bedding	Mju	280	35	SW	
115	bedding	Mju	300	34	SW	
116	bedding	Dsi	285	21	SW	
117	bedding	Dg	295	16	SW	

APPENDIX D: FIELD DATA AND AREA STOP/MEASUREMENT LOCATION MAP

Stop number	Feature	Map Unit	Az°/ Trend°	Dip°/ Plunge°	Dip D	Comments
118	bedding	Dg	280	9	SW	
119	bedding	Dg	290	4	SW	
120	bedding	Opa	310	27	NE	
121	bedding	Oe	322	25	SW	
122	bedding	Mju	85	19	NW	
123	bedding	Dg	299	35	SW	
124	bedding	Dg	282	28	SW	
125	bedding	Opg	290	44	NE	
126	bedding	Opg	0	70	E	
127	bedding	Opg	306	49	NE	
128	bedding	Opa	320	50	NE	
129	fault	Opg	8	68	E	SPFZ
130	bedding	Dsi	85	86	N	
131	bedding	Opg	327	50	SW	
132	fault	Opg	95	30	NE	
133	bedding	Opg	315	44	SE	
134	bedding	Mju	295	34	SW	
135	bedding	Mju	355	31	SW	
136	fault	Mju	73	72	SE	Tunnel Springs fault
137	fault	Mju	303	40	SW	cross fault Tunnel Springs fault
138	bedding	Mjl	40	72	NW	
139	bedding	Opa	330	57	NE	
140	fold	Opa	324	63	NE	
141	fault	Opa	62	58	SE	
142	fold	Opa	321	43	NE	
143	fault	Opa	40	68	SE	
144	bedding	Dg	142	51	NE	
145	bedding	Dg	100	44	SW	
146	fault		133	60	SW	Lincoln thrust surface
147	bedding	Dg	328	45	NE	

APPENDIX D: FIELD DATA AND AREA STOP/MEASUREMENT LOCATION MAP

Stop number	Feature	Map Unit	Az◦/ Trend◦	Dip◦/ Plunge◦	Dip D	Comments
148	bedding	Dsi	141	36	NE	
149	bedding	Opa	307	34	NE	
150	bedding	Opa	129	37	NE	
151	bedding	Opa	293	48	NE	
152	bedding	Opa	304	36	NE	
153	bedding	lPe	348	40	NE	
154	bedding	lPe	354	46	NE	
155	bedding	lPe	326	42	NE	
156	bedding	lPe	295	28	E	
157	bedding	lPe	9	33	E	
158	fault	lPe	149	57	SW	SPFZ lPe/Єl
159	bedding	Mc	154	88	SW	
160	bedding	Mc	103	67	NE	
161	bedding	Msw	179	71	SW	
162	bedding	Dg	80	53	NW	
163	bedding	Dg	337	67	E	
164	bedding	Dg	154	50	W	
165	bedding	Dg	70	40	N	
166	bedding	Dg	197	38	W	
167	bedding	Mjl	65	65	W	
168a	bedding	Dg	187	35	W	
168b	fault	Dg	148	11	SW	Schofield thrust fault surface
169	bedding	Єu	20	30	E	
170	bedding	Єl	7	46	E	
171	bedding	Єl	345	19	E	
172	bedding	Єu	10	43	E	
173	bedding	Opg	337	45	E	
174	bedding	Opg	352	46	E	
175	bedding	Opg	341	35	E	
176	bedding	Opg	322	28	E	

APPENDIX D: FIELD DATA AND AREA
STOP/MEASUREMENT LOCATION MAP

Stop number	Feature	Map Unit	Az°/ Trend°	Dip°/ Plunge°	Dip D	Comments
177	bedding	Єu	346	24	E	
178	bedding	Dg	318	58	W	
179	bedding	Mjl	348	54	W	
180	bedding	Oe	340	62	W	
181	bedding	Opa	293	50	E	
182	bedding	Opa	52	38	E	
183	bedding	Oe	18	64	W	
184	bedding	Oe	340	37	W	
185	bedding	Mjl	349	22	W	
186	bedding	Mju	8	68	E	
187	bedding	Mjl	42	47	E	
188	bedding	Dg	44	46	E	
189	bedding	Dg	20	48	E	

APPENDIX D: FIELD DATA AND AREA STOP/MEASUREMENT LOCATION MAP

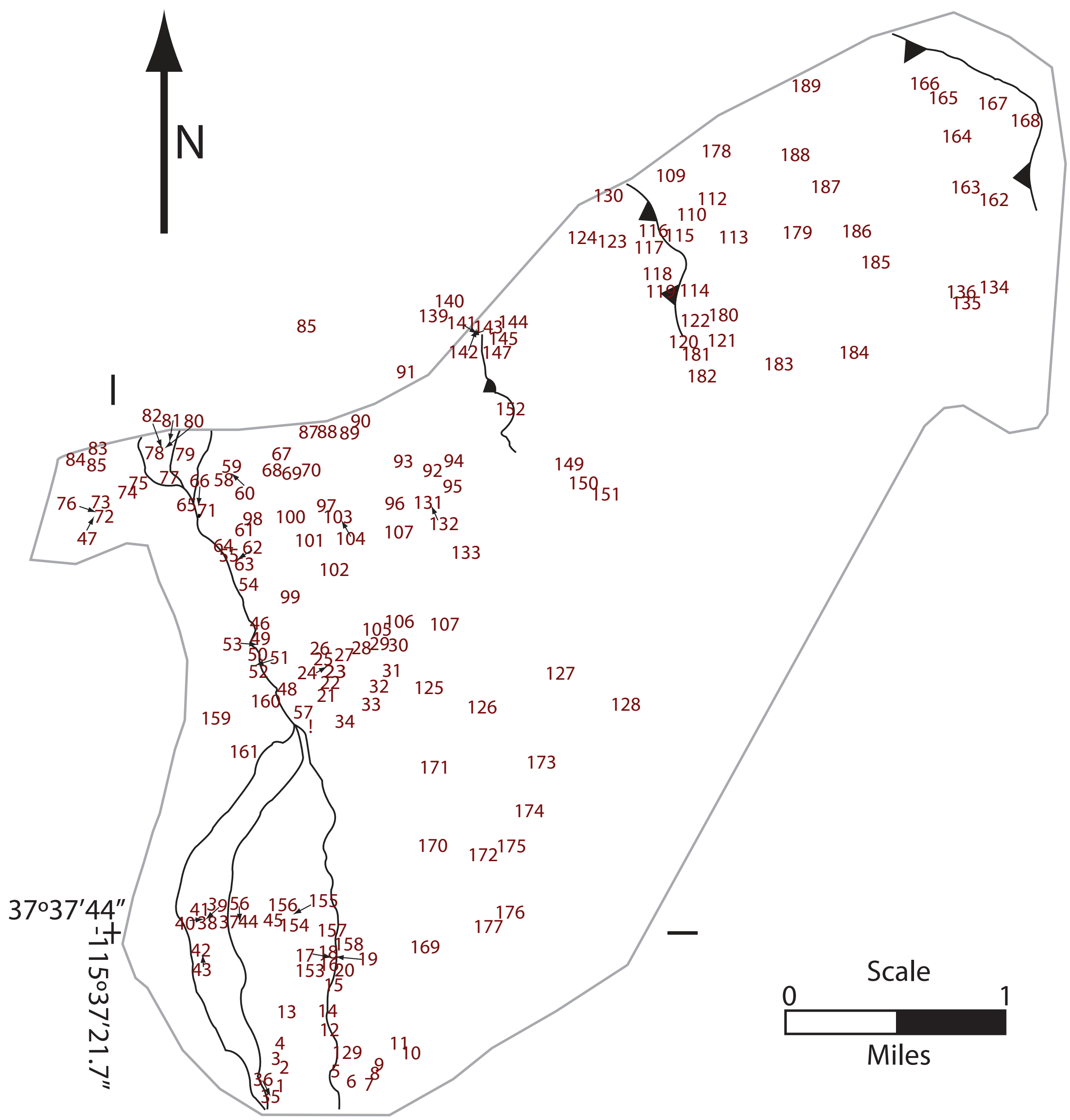

*The GPS coordinates shown are from Chocolate Drop, a landmark in Lincoln County.

APPENDIX E: PLATE 1 GEOLOGIC MAP
OF THE WESTERN TIMPAHUTE RANGE

ATTACHMENT

APPENDIX F: PLATE 2 CROSS SECTIONS OF THE WESTERN TIMPAHUTE RANGE

ATTACHMENT

REFERENCES

Allmendinger, R. W., and Jordan, T. E., 1984, Mesozoic structure of the Newfoundland Mountains, Utah: Horizontal shortening and subsequent extension in the hinterland of the Sevier belt: Geological Society of America Bulletin, v. 95, p. 1280-1292.

Armstrong, R. L., 1968, Sevier orogenic belt in Nevada and Utah: Geological Society America Bulletin, v. 79, p. 429-458.

Armstrong, R. L., 1972, Low-Angle (Denudation) faults, hinterland of the Sevier orogenic belt, eastern Nevada and western Utah: Geological Society of America Bulletin, v. 83, p. 1729-1754.

Armstrong, P. A., and Bartley, J. M., 1993, Displacement and deformation associated with a lateral thrust termination, southern Golden Gate Range, southern Nevada, U.S.A.: Journal of Structural Geology, v. 15, p. 721-735.

Axen, G. J., Wernicke, B. P., Skelly, M. F., and Taylor, W. J., 1990, Mesozoic and Cenozoic tectonics of the Sevier thrust belt in the Virgin River Valley area, southern Nevada, *in* Wernicke, B. P., ed., Basin and Range extensional tectonics near the latitude of Las Vegas, Nevada: Boulder, Colorado, Geological Society of America Memoir 176, p. 123-153.

Axen, G. J., Taylor, W. J., and Bartley, J. M., 1993, Space-time patterns and tectonic controls of Tertiary extension and magmatism in the Great Basin of the western United States: Geological Society of America Bulletin, v. 105, p. 56-76.

Barnes, H, E. B. Ekren, C. L. Rodgers, and D. C. Hedland, 1982, Geologic and tectonic maps of the Mercury Quadrangle, Nye and Clark Counties, Nevada, U.S. Geological Survey Miscellaneous Investigations, Map I-1197.

Bartley, J. M., and Gleason, G., 1990, Tertiary normal faults superimposed on Mesozoic thrusts, Quinn Canyon and Grant Ranges, Nye County, Nevada, *in* Wernicke, B. P., ed., Basin and Range extensional tectonics near the latitude of Las Vegas, Nevada: Boulder, Colorado, Geological Society of America Memoir 176, p. 195-212.

Bartley, J. M., Axen, G. J., Taylor, W. J., and Fryxell, J. E., 1988, Cenozoic tectonics of a transect through eastern Nevada near 38 degrees N latitude *in* This Extended Land, Geological Journeys in the Southern Basin and Range, Weide, D. L. and Faber, M. L., eds, Geological Society of America, Cordilleran Section, Field Trip Guidebook, p. 1-20.

Barton, M. D., 1990, Cretaceous magmatism, metamorphism, and metallogeny in the east-central Great Basin, *in* The Nature and Origin of Cordilleran Magmatism Anderson, J. L., ed.,: Geological Society of America Memoir 174, p. 283-302.

Best, M. G., and Christensen, E. H., 1991, Limited extension during peak Tertiary volcanism, Great Basin of Nevada and Utah: Journal of Geophysical Research, v. 96, p. 13509-13528.

Best, M. G., Christiansen, E. H., and Blank, H. R., 1989, Oligocene caldera complex and calc-alkaline tuffs and lavas of the Indian Peak volcanic field, Nevada and Utah: Geological Society of America Bulletin, v. 101, p. 1076-1090.

Best, M. G., Scott, R. B., Rowley, P. D., Swadley, W. C., Anderson, R. E., Gromme, C. S., Harding, A. E., Deino, A. L., Christensen, E. H., Tingey, D. G., and Sullivan, K. R., 1993, Oligocene-Miocene caldera complexes, ash-flow sheets, and tectonism in the central and southeastern Great Basin, *in* Lahren, M. M., et al., eds., Crustal Evolution of the Great Basin and Sierra Nevada: Reno, Nevada, University of Nevada-Reno, Field Trip Guidebook: p. 285-311.

Bidgoli, T. S., 2005, The Role of Transverse Faults in Great Basin Extension: Transfer Faults or N-S Extension? [M.S. thesis]: Las Vegas, University of Nevada Las Vegas, 111 p.

Bohannon, R. G., and Parsons, T., 1995, Tectonic implications of post-30 Ma Pacific and North American relative plate motions: Geological Society of America Bulletin, v. 107, p. 937-959.

Boyer, S. E., and Elliot, D., 1982, Thrust Systems: American Association of Petroleum Geologists Bulletin, v. 66, p. 1196-1230.

Burchfiel, B. C., and Davis, G. A., 1972, Structural framework and evolution of the southern part of the Cordilleran orogen, western United States: American Journal of Science, v. 272, no. 2, p. 97-118.

Burchfiel, B. C., Cowan, D. S., and Davis, G. A., 1992, Tectonic overview of the Cordilleran orogen in the western United States, *in* Burchfiel, B. C., Lipman, P. W., and Zoback, M. L., eds., The Cordilleran orogen: Conterminous U.S.: Boulder, Colorado, Geological Society of America, Geology of North America, v. G-3, p. 407-479.

Cashman, P., Trexler, J., Snyder, W., Davydov, V., and Taylor, W., 2008, Late Paleozoic deformation in central and southern Nevada, *in* Duebendorfer, E. M., and Smith, E. I., eds., Field Guide to plutons, volcanoes, faults, reefs, dinosaurs, and possible glaciation in selected areas of Arizona, California, and Nevada: Geological Society of America Field Guide 11, p. 21-42.

Cashman, P. H., Villa, D. E., Taylor, W. J., Davydov, V. I., and Trexler, J. H., 2011, Late Paleozoic contractional and extensional deformation at Edna Mountain, Nevada: Geological Society of America Bulletin, v. 123, p. 651-668.

Caskey, S. J., and Schweickert, R. A., 1992, Mesozoic deformation in the Nevada Test site and vicinity: Implications for the structural framework of the Cordilleran fold and thrust belt and Tertiary extension north of Las Vegas Valley: Tectonics, v. 11, p. 1314-1331.

Cole, J. C., and Cashman, P. H., 1999, Structural relationships of pre-Tertiary rocks in the Nevada Test Site region, southern Nevada: U.S. Geological Survey Professional Paper 1607, 39 p.

Cole, J. C., Harris, A. G., Lanphere, M. A., Barker, C. E., and Warren, R. G., 1993, The case for pre-middle Cretaceous extensional faulting in northern Yucca Flat, southwestern Nevada: Geological Society of America Abstracts with Programs, v. 25, p. 22.

Compton, R. R., 1985, Geology in the Field, John Wiley & Sons, Inc., 398 p.

Cowan, D. S., and Bruhn, R. L., 1992, Late Jurassic to early Late Cretaceous geology of the U.S. Cordillera, Tectonic overview of the Cordilleran orogen in the western

United States, *in* Burchfiel, B. C., Lipman, P. W., and Zoback, M. L., eds., The Cordilleran orogen: Conterminous U.S.: Boulder, Colorado, Geological Society of America, Geology of North America, v. G-3, p. 169-203.

Dahlstrom, C. D. A., 1969, Balanced cross sections: Canadian Journal of Earth Sciences, v. 6, p. 57-71.

DeCelles, P. G., 2004, Late Jurassic to Eocene evolution of the Cordilleran thrust belt and foreland basin system, western U.S.A: American Journal of Science, v. 304, p. 105-168.

DeCelles, P. G., and Coogan, J. C., 2006, Regional structure and kinematic history of the Sevier fold-and-thrust belt, central Utah: Geological Society of America Bulletin, v. 118, p. 841-864.

DeCelles, P. G., Lawton, T. F., and Mitra, G., 1995, Thrust timing, growth of structural culminations, and synorogenic sedimentation in the type area of the Sevier orogenic belt, central Utah: Geology, v. 23, p. 699-702.

Dickinson, W. R., 2006, Geotectonic evolution of the Great Basin: Geosphere, v. 2, p. 353-368.

DuBray, E. A., 1986, Mineral Resources, Geology, and Geophysics of the Worthington Mountains Wilderness Study Area, Lincoln County, Nevada: U.S. Geological Survey Bulletin 1728, p. A1-A11.

Eaton, G. P., 1982, The Basin and Range Province: Origin and Tectonic Significance: Annual Review of Earth and Planetary Sciences, v. 10, no. 1, p. 409-440.

Ekren, E. B., Bucknam, R. C., Carr, W. J., Dixon, G. L., and Quinlivan, W. D., 1976, East-trending lineaments in central Nevada: U.S. Geological Survey Professional Paper 986, 19 p.

Ekren, E. B., Orkild, P. P., Sargent, K. A., and Dixon, G. L., 1977, Geologic map of Tertiary Rocks, Lincoln County, Nevada: U.S. Geological Survey Miscellaneous Investigations Series, Map I-1041, scale 1:250,000.

Faulds, J. E., and Varga, R. J., 1998, The role of accommodation zones and transfer zones in the regional segmentation of extended terranes: Geological Society of America Special Papers 323, p. 1-45.

Fryxell, J. E., 1988, Geologic map and description of stratigraphy and structure of the west-central Grant Range, Nye County, Nevada: Geological Society of America Map and Chart Series MCH064, 16 p., scale 1:24,000.

Gans, P. B., Manhood, G. A., and Schermer, E., 1989, Synextensional magmatism in the Basin and Range Province; A case study from the eastern Great Basin: Geological Society of America Special Paper 233, 53 p.

Gans, P. B., and Bohrson, W. A., 1998, Suppression of volcanism during rapid extension in the Basin and Range Province, United States: Science, v. 279, p. 66-68.

Gillespie, P. A., Walsh, J. J., and Watterson, J., 1992, Limitations of dimension and displacement data from single faults and the consequences for data analysis and interpretation: Journal of Structural Geology, v. 14, p. 1157-1172.

Greene, D. C., Schweickert, R. A., and Stevens, C. H., 1997, The Northern Ritter Range pendant, eastern Sierra Nevada California Roberts Mountains allochthon and the western margin of the Cordilleran miogeocline: Geological Society of America Bulletin, v. 109, p. 1294-1305.

Groshong, R. H., 1989, Half-graben structures; balanced models of extensional fault-bend folds: Geological Society of America Bulletin, v. 101, p. 96-105.

Guth, P. L., 1981, Tertiary extension north of the Las Vegas Valley shear zone, Sheep and Desert Ranges, Clark County, Nevada, Geological Society of America Bulletin, v. 92, p. 763-771.

Guth, P. L., 1990, Superimposed Mesozoic and Cenozoic deformation, northwestern Clark County, Nevada, i*n* Wernicke, B. P., ed., Basin and Range extensional tectonics near the latitude of Las Vegas, Nevada: Geological Society of America Memoir 176, p. 237-249.

Hodges, K. V., and Walker, J. D., 1992, Extension in the Cretaceous Sevier orogen, North American Cordillera: Geological Society of America Bulletin, v. 104, p. 560-569.

Jayko A. S., 1990, Shallow crustal deformation in the Pahranagat area, southern Nevada, *in* Wernicke, B. P., ed., Basin and Range extensional tectonics near the latitude of Las Vegas, Nevada: Boulder, Colorado, Geological Society of America Memoir 176, p. 213-236.

Kellog, H. E., 1964, Cenozoic stratigraphy and structure of the southern Egan Range, Nevada: Geological Society of America Bulletin, v. 75, p. 949-968.

Krueger, H. W., and Schilling, J. H., 1971, Geochron/ Nevada Bureau of Mines K/Ar age determinations- List 1, Isochron West, v. 1, p. 9-14.

Long, S. P., 2012, Magnitudes and spatial patterns of erosional exhumation in the Sevier hinterland, eastern Nevada and western Utah, USA: Insights from a Paleogene paleogeologic map: Geosphere, v. 8, p. 881-901.

Martin, M. W., 1987, Geology of the Worthington Mountains, Lincoln County, Nevada [M.S. thesis]: Chapel Hill, University of North Carolina, 112 p.

Miller, E. L., Miller, M. M., Stevens, C. H., Wright, J. E., and Madrid, R., 1992, Late Paleozoic paleogeography and tectonic evolution of the western U.S. Cordillera, *in* Burchfiel, B. C., Lipman, P. W., and Zoback, M. L., eds., The Cordilleran Orogen: Conterminous U.S.: The Geology of North America, Volume G-3, Decade of North American Geology: Boulder, Colorado, Geological Society of America, p 57-106.

Nolan, T. B., Merriam, C. W., and Williams, J. S., 1956, The stratigraphic section in the vicinity of Eureka, Nevada: U.S. Geological Survey Professional Paper 276, 77 p.

Oldow, J. S., 1983, Tectonic implications of a late Mesozoic fold and thrust belt in northwestern Nevada: Geology, v. 11, p. 542-546.

Oldow, J. S., 1984, Spacial variability in the structure of the Roberts Mountains allochthon, western Nevada: Geological Society of America Bulletin, vol. 95, p. 174-185.

Peacock, D. C. P. and Sanderson, D. J., 1991, Displacements, segment linkage and relay ramps in normal fault zones: Journal of Structural Geology, vol. 13, p. 721-733.

Pinto, J. A. and Warme, J. E., 2008, Alamo event, Nevada; Crater stratigraphy and impact breccia realms, *in* Evans, K. R., Horton, J. W., Jr., King, D. T., Jr., and Morrow, J. R., eds., The Sedimentary Record of Meteorite Impacts: Geological Society of America Special Paper 437, p. 99-137.

Poole, F. G., 1974, Flysch deposits of the Antler foreland basin, western United States, *in* Dickinson, W. R., ed., Tectonics and sedimentation: Society of Economic Paleontologists and Mineralogists Special Publication 22, p. 58-82.

Renik, B., and Christie-Blick, N., 2013, A new hypothesis for the amount and distribution of dextral displacement along the Fish Lake Valley - northern Death Valley - Furnace Creek fault zone, California - Nevada: Tectonics, v. 32, p. 1-23.

Reso, A., 1963, Composite columnar section of expose Paleozoic and Cenozoic rocks in the Pahranagat Range, Lincoln County, Nevada, Geological Society of America Bulletin, v. 74, p. 901-918.

Roberts, R. J., Hotz, P. E., Gilluly, J., and Ferguson, H. G., 1958, Paleozoic rocks of north-central Nevada: American Association of Petroleum Geologists Bulletin, v. 42, p. 2813– 2857.

Ross, R. J., 1964, Middle and Lower Ordovician formations in southernmost Nevada and adjacent California: U.S. Geological Survey Bulletin, p. C1-C101.

Rowley, P. D., 1998, Cenozoic transverse zones and igneous belts in the Great Basin, western United States: Their tectonic and economic implications, *in* Faulds, J. E., and Stewart, J. H., eds., Accommodation Zones and Transfer Zones: The Regional Segmentation of the Basin and Range Province: Boulder, Colorado, Geological Society of America Special Paper 323, p. 195-228.

Saller, A. H., and Dickinson, W. R., 1982, Alluvial to marine facies transition in the Antler overlap sequence, Pennsylvanian and Permian of north-central Nevada: Journal of Sedimentary Petrology, v. 52, p. 925-940.

Sandru, J. M., and Taylor, W. J., 2003, Cenozoic extension and strike-slip tectonics in the Mt. Irish Range, Nevada; Changes in stress fields through time: GSA Abstracts with programs, v. 35, no. 6, p. 26.

Schmitt, A. K., Grove, M., Harrison, T. M., Lovera, O., Hulen, J., and Walters, M., 2003, The Geysers-Cobb Mountain Magma System, California (Part 1): U-Pb zircon ages of volcanic rocks, conditions of zircon crystallization and magma residence times: Geochimica et Cosmochimica Acta, v. 67, p. 3423-3442.

Severinghaus, J., and Atwater, T., 1990, Cenozoic geometry and thermal state of the subducting slabs beneath western North America, *in* Wernicke, B. P., ed., Basin and Range extensional tectonics near the latitude of Las Vegas, Nevada: Boulder, Colorado, Geological Society of America Memoir 176, p. 1-22.

Siebenaler, S. A., 2010, Late Paleozoic deformation in the Osgood Mountains and Dry Hills, Northern Nevada [M.S. thesis]: Las Vegas, University of Nevada Las Vegas, 165 p.

Snow, J. K., 1992, Large magnitude Permian shortening and continental-marginal tectonics in the southern Cordillera: Geological Society of America Bulletin, v. 104, p. 80-105.

Snow, J. K., and Wernicke, B. P., 1989, Uniqueness of geological correlations; an example from the Death Valley extended terrain: Geological Society of America Bulletin, v. 101, p. 1351-1362.

Speed, R. C., 1983, Evolution of the sialic margin in the central-western United States, in Watkins, J. S., and Drake, C. L., eds., Studies in Continental Margin Geology: American Association of Petroleum Geologists Memoir 34, p 457-468.

Speed, R. C., and Sleep, N. H., 1982, Antler Orogeny and foreland basin; a model: Geological Society of America Bulletin, v. 93, p. 815-828.

Speed, R. C., Elison, M. W., and Heck, F. R., 1988, Phanerozoic tectonic evolution of the Great Basin, in Ernst, W. G., ed., Metamorphism and crustal evolution of the western United States, Rubey Volume 7: Englewood Cliffs, New Jersey, Prentice-Hall, p. 572-605.

Stewart, J. H., 1971, Basin and Range structure: a system of horsts and grabens produced by deep-seated extension: Geological Society of America Bulletin, v. 82, p. 1019-1044.

Stewart, J. H., 1980, Geology of Nevada, a discussion to accompany the geologic map of Nevada: Nevada Bureau of Mines and Geology Special Publication 4, 136 p.

Taylor, W. J., 1990, Spatial and temporal relations of Cenozoic volcanism and extension in the North Pahroc and Seaman Ranges, eastern Nevada, *in* Wernicke, B. P., ed., Basin and Range extensional tectonics near the latitude of Las Vegas, Nevada: Boulder, Colorado, Geological Society of America Memoir 176, p. 181-193.

Taylor, W. J., and Bartley, J. M., 1992, Prevolcanic extensional Seaman breakaway fault and its geologic implications for eastern Nevada and western Utah: Geological Society of America Bulletin, v. 104, p. 255-266.

Taylor, W. J., and Switzer, D. D., 2001, Temporal changes in fault strike (to 90 degrees) and extension directions during multiple episodes of extension: An example from eastern Nevada: Geological Society of America Bulletin, v. 113, p. 743-759.

Taylor, W. J., Bartley, J. M., Lux, D. R., and Axen, G. J., 1989, Timing of Tertiary Extension in the Railroad Valley-Pioche Transect, Nevada: Constraints from $^{40}Ar/^{39}Ar$ ages of volcanic rocks: Journal of Geophysical Research, v. 94, p. 7757-7774.

Taylor, W. J., Bartley, J. M., Fryxell, J. E., Schmitt, J. G., and Vandervoot, D. S., 1993, Tectonic style and regional relations of the central Nevada thrust belt, in Lahren, M. N., Trexler, J. H., Jr., and Spinosa, C., eds., Crustal Evolution of the Great Basin and Sierra Nevada: Cordilleran/ Rocky Mountain Section, Geological Society of America Field Trip Guidebook, University of Nevada, Reno, p. 57-96.

Taylor, W. J., Bartley, J. M., Martin, M. W., Geissman, J. W., Walker, J. D., Armstrong, P. A., and Fryxell, J. E., 2000, Relations between hinterland and foreland shortening: Sevier orogeny, central North American Cordillera: Tectonics, v. 19, p. 1124-1143.

Tingley, J. V., 1991, Mineral resources of the Timpahute Range 30’ x 60’ quadrangle: Nevada Bureau of Mines and Geology Report 46, 40 p.

Trexler, J. H., Jr., Cashman, P. H., Snyder, W. S., and Davydov, V. I., 2004, Late Paleozoic tectonism in Nevada: Timing, kinematics, and tectonic significance: Geological Society of America Bulletin, v. 116, p. 525-538.

Tschanz, C. M., and Pampeyan, E. H., 1970, Geology and mineral deposits of Lincoln County, Nevada: Nevada Bureau of Mines and Geology Bulletin 73, 188 p.

Vandervoort, D. S., and Schmitt, J. G., 1990, Cretaceous to early Tertiary paleogeography in the hinterland of the Sevier thrust belt, east-central Nevada: Geology, v. 18, p. 567-570.

Villa, D. E., 2007, Late Paleozoic deformation at Edna Mountain, Humboldt County, Nevada [M.S. thesis]: University of Nevada, Reno, 106 p.

Wallace, R. E., 1984, Patterns and timing of Late Quaternary faulting in the Great Basin Province and relation to some regional tectonic features: Journal of Geophysical Research, v. 89, p. 5763-5769.

Wells, M. L., Dallmeyer, R. D., and Allmendinger, R. W., 1990, Late Cretaceous extension in the hinterland of the Sevier thrust belt, northwestern Utah and southern Idaho: Geology, v. 18, p. 929-933.

Wells, M. L., Hoisch, T. D., Peters, M. T., Miller, D. M., Wolff, E. D., and Hanson, L. M., 1998, The Mahogany Peaks Fault, a Late Cretaceous-Paleocene(?) Normal Fault in the Hinterland of the Sevier Orogen: Journal of Geology, v. 106, p. 623-634.

Wernicke, B., 1992, Cenozoic extensional tectonics of the U.S. Cordillera, *in* Burchfiel, B. C., Lipman, P. W., and Zoback, M. L., eds., The Cordilleran orogen: Conterminous U.S.: Boulder, Colorado, Geological Society of America, Geology of North America, v. G-3, p. 553-581.

Wernicke, B. P., Axen, G. J., and Snow, J. K., 1988, Basin and Range extensional tectonics at the latitude of Las Vegas, Nevada: Geological Society of America Bulletin, v. 100, p. 1738-1757.

Wyld, S. J., 2002, Structural evolution of a Mesozoic backarc fold-and-thrust belt in the U.S. Cordillera: New evidence from northern Nevada: Geological Society of America Bulletin, v. 114, p. 1452-1468.

Wyld, S. J., Rogers, J. W., and Wright, J. E., 2001, Structural evolution within the Luning-Fencemaker fold-thrust belt, Nevada: progression from back-arc basin closure to intra-arc shortening: Journal of Structural Geology, v. 23, p. 1971-1995.

Wyld, S. J., Rogers, J. W., and Copeland, P., 2003, Metamorphic evolution of the Luning-Fencemaker fold-thrust belt, Nevada: Illite crystallinity, metamorphic petrology, and $^{40}Ar/^{39}Ar$ Geochronology: The Journal of Geology, v. 111, p. 17-38.

Yonkee, W. A., 1992, Basement-cover relations, Sevier orogenic belt, northern Utah: Geological Society of America Bulletin, v. 104, p. 280-302.

VITA

Graduate College
University of Nevada, Las Vegas

Angela Giovanna Russo
russoa4@gmail.com

Education:

Master of Science, Geoscience 2013
University of Nevada, Las Vegas
Thesis Title: Pennsylvanian to Cretaceous fold and thrusts in south-central Nevada: Evidence from the Timpahute Range
Advisor: Dr. Wanda J. Taylor

Bachelor of Science, Geology 2007
Northern Kentucky University
Thesis Title: Clay Mineralogy and Petrology Associated with a Dinosaur Lake (Aaron Scott Quarry, Morrison Formation, Jurassic), Utah
Advisor: Dr. Janet L. Bertog

Work Experience:

Project Geologist, Klondex Mines Ltd., Elko, NV, 2013
Mine Geologist, Great Basin Gold Ltd., Winnemucca, NV, 2010-13
Teaching Assistant, Geoscience Department, UNLV, Las Vegas, NV, 2007-10
Dinosaur Dig, Cincinnati Museum Center, Mother's Day Site, MT, 2007
Paleolab Technician, Cincinnati Museum Center, Cincinnati, OH, 2006-07
Dinosaur Dig, Cincinnati Museum Center, Aaron Scott Quarry, UT, 2006-07

Publications:

Russo, A. G. and Rowland, S. M., 2008, Paleoecology of a Rancholabrean community preserved in floodplain deposits of Meadow Valley Wash, Lincoln County, Nevada: Geological Society of America, Cordilleran/Rockly Mountain Section, Las Vegas, v. 40, no. 1, p. 12.

Russo, A., Robinson, R., Moore, J., Bertog, J. L., and Jeffrey, D. L., 2006, Clay mineralogy associated with a dinosaur lake (Aaron Scott Quarry, Morrison Formation, Jurassic), Utah: Kentucky Academy of Science abstract, p. 50.

Thesis Examination Committee:

Chairperson, Wanda Taylor, Ph.D.
Committee Member, Eugene Smith, Ph.D.
Committee Member, Ganqing Jiang, Ph.D.
Graduate Faculty Representative, Lon Spight, Ph.D.